Winter 12-1976

Longitudinal Stress Wave Propagation in Long Bone

Richard R. Pelker
Yale University.

LONGITUDINAL STRESS WAVE PROPAGATION IN LONG BONE

A Dissertation

Presented to the Faculty of the Graduate School

of

Yale University

in Candidacy for the Degree of

Doctor of Philosophy

by

Richard R. Pelker

December 1976

ABSTRACT

LONGITUDINAL STRESS WAVE PROPAGATION IN LONG BONE

Richard R. Pelker

Yale University 1976

Compressive impact tests were performed on human long bone with the aim of accumulating information about the wave propagation characteristics of bone for clinical use and to increase our understanding of osseous tissue. Dynamic tests on intact bone were carried out by impacting one end of dissected bone specimens and recording the stress wave pulses by means of strain gages and a magnetic velocitometer that was constructed for this study using skeletal traction pins. After the initial set of studies were completed, serial cuts were made into the bone cortex at increasing depths as an attempt to model healing bone fracture. The above wave propagation studies were then repeated to measure the transmission coefficient through the fracture and any change in wave character due to the fracture.

In conjunction with this, human long bone was mathematically modeled as a poroelastic hollow cylinder. A computer simulation was devised to provide numerical results from the theory and an attempt was made to correlate the experimental findings with the model's predictions for various porosities.

to my parents,

Eugene and Violet Pelker

who never sought anything of me,
but believe in me just the same.

ACKNOWLEDGEMENTS

If this work is viewed to be faulty or inferior in any manner its deficiencies are solely the author's responsibility. If, on the other hand, it proves to be of some worth, scientific or otherwise, the author wishes to express his gratitude to all who helped in its formulation, preparation or execution. He would especially like to acknowledge the aid of the following:

Professor Subrata Saha, my advisor, for his time, advice and expertise and without whose aid this project would not have been possible.

Professors James A. Albright, B.T. Chu and A. Phillips for kindly consenting to serve on the thesis committee for this work.

Doctor Thomas Johnson's inspiration and guidance is especially appreciated by the author.

The expertise of Mrs. Gertrude Chaplin in preparing the microscopic sections and photographs is humbly recognized.

Mr. A. Agostinelli for the instruction and use of the photodensitometer.

Professor H. Stark for the use of the image analyser.

Miss Gail Martin for typing this manuscript.

The financial support of Yale University and the Medical Scientist Training Program during this research is also appreciated.

TABLE OF CONTENTS

LIST OF TABLES

LIST OF ILLUSTRATIONS

Chapter I

INTRODUCTION

PURPOSE

The investigation of the mechanical properties of bone dates back to the time of Galileo, and numerous studies since that time have greatly increased our basic understanding of the biomechanics of the musculoskeletal system. However the vast majority of these tests have been destructive studies and therefore are of limited clinical usefulness. The numerous possible applications for a nondestructive technique include the monitoring of fracture healing, the quantization of osteoporosis in elderly individuals or in patients with metabolic bone disease and the evaluation of treatment in such patients.

Possibly the stress wave propagation properties of bone could provide the basis for a noninvasive test since these are dependent on its basic biomechanical characteristics. Although there have been several recent

studies of the dynamic properties of hard tissue, much more is known about its static properties. Therefore, before this type of noninvasive test becomes practical, the dynamic response of bone must be better understood. This is the major aim of this work.

THEORY - LONGITUDINAL WAVES IN RODS

The elementary theory that approximately describes the propagation of longitudinal waves in an elastic rod has been studied extensively and is well known (Kolsky 1963, Parson 1959, Timoshenko and Goodier 1970). The wave equation resulting from this theory is the well known formula:

$$\frac{\partial^2 \sigma_x}{\partial t^2} = c_o^2 \frac{\partial^2 \sigma_x}{\partial x^2} \tag{1.1}$$

where:

σ_x = axial stress along the x direction

t = time

x = axial coordinate

c_o = elastic wave velocity = $\sqrt{E/\rho}$

E = Young's modulus

ρ = mass density

The basic assumptions of this approximation are:

a) each plane cross section of the rod remains coplanar during deformation.

b) the distribution of stress, strain and particle velocity are

uniform over each cross section.

The general solution to this equation can be expressed as

$$\sigma_x = f(x - ct) + F(x + ct)$$

where f and F are arbitrary functions that are determined by the initial conditions, the first corresponding to a wave traveling in the positive x direction, the latter to a wave traveling in the reverse direction.

For the particular case of an infinitely long rod a solution to equation 1.1 is:

$$\sigma_x = \sigma_0 \quad \exp{-i} \frac{2\pi}{\lambda} (x - ct)$$

where λ is the wavelength and c is the velocity of the wave. It is to be noted that the velocity of the wave in this elementary theory has no dependence on the wave length. Therefore, since any wave can be described as a Fourier sum of such waves each contributing part will be propagated at the same velocity, c_o and thus there will be no distortion of the wave form as it is propagated down the bar.

By using more exact theories a more accurate description of the phenomena can be obtained. Pochhammer (1876) and Chree (1899) independently developed the theory further, including the contribution of the Poisson effect. They showed that the wave velocity was dependent on the ratio of the rod radius to wavelength and on Poisson's ratio. Thus in this more comprehensive theory the Fourier components of a wave pulse would each travel at a different velocity. The pulse would then become distorted as it propagated down the rod. Mindlin and Herrmann (1951) included the effects of shearing stress and strains on stress wave propagation in a

bar. However, David (1948) showed that if the ratio of rod radius to wavelength is small then the elementary theory rrovides an adequate description.

Much work has been done extending these rather basic theories to more specific cases by varying the geometries considered. The case of a hollow elastic rod has been studies by Gasiz (1959a,b), Fitch (1963), Chong et al. (1969), and Perinca (1973). The problem has been further perturbed by considering the bar as a hollow thin shell by Herrmann and Mirsky (1956) and as a multilayered cylinder by Whittier and Jones (1967), Reuter (1968), Chou (1968), and Armenakas (1967). Miklowitz (1957) described the propagation of a wave in inhomogeneous cylinders. Several authors have considered the case of a noncylindrical rod with varying cross-sections (Tanaka and Kurokawa 1973, Wong, et al. 1966, Lee and Sechler 1975, Handelman and Rubenfeld 1972, and Habberstad 1971).

Besides considering varying geometries many authors (Wu and Sackman 1974, Bartholomew and Torvik 1972, Benveniste and Lubliner 1972, and Yuan and Lianis 1974) have considered the problem where the bar is no longer a simple elastic material, but is viscoelastic or nonlinear in its properties. Several years ago Biot developed a theory of stresses in a porous material. This has been the focus of several papers since that time (Biot 1956a,b, Biot and Willis 1957, Biot 1961, Lubinski 1955, Mallik and Ghosh 1974, Sve 1973, Trofimov, et al. 1968, Jones 1969, Hoffman, et al. 1968, Jones 1961, Nowinski and David 1971, and Pelker and Saha 1975).

A few authors have examined the problem of a discontinuity in the

cross-section on wave propagation. Kenner and Goldsmith (1968) and Habberstad and Hoge (1971) have considered the case of a discontinuity that is short compared to the wavelength of the pulse, which simplifies the problem of computing the transmission and reflection coefficients.

It can be seen from this cursory overview of the field that the area of stress wave propagation has been extensively studied. However, it will also be noted by the presence of recent work that continued interest exists especially with respect to different geometries and nonelastic materials.

MECHANICAL PROPERTIES OF BONE

Static Properties

The mechanical properties of bone has been the subject of investigation for numerous years with the first contribution to the literature being attributed to Wertheim (1847). The literature in the area has been the subject of several reviews where the pertinent information is collected. Among these are Evans (1957) who extensively reviewed the early work in the field. Yamada (1970), Currey (1970), Swanson (1971) and Ascenzi and Bell (1972) have reviewed much of the literature since then. The modulus of elasticity along with the ultimate breaking strength are two of the more widely studied properties. A summary of some of the experimental work may be found in Tables 1.1 - 1.3. It can be seen from these results that bone is approximately twice as strong in compression as in tension. The ulti-

Table 1.1

Modulus of Elasticity[1]

Author	Species	Bone	E (kg/cm^2)
Ascenzi and Bonucci (1968)	Man	Femur	49,100-94,900
Ascenzi and Bonucci (1967)	Man	Femur	39,600-119,000
	Ox	Femur	54,600-169,000
Bird, et al. (1968)	Ox	Femur	214,000 Longitudinal 162,000 Circumferential 68,000 Radial
Currey (1969a)	Rabbit	Meta-tarsal	60,000-170,000
Dempster and Liddicoat (1952)	Man	Femur, tibia	88,700 Longitudinal 42,700 Circumferential 38,400 Radial
			145,000 Compression 123,000 Tension
Evans and Bang (1967)	Man	Femur	144,000
		Tibia	155,000
		Fibula	169,000
Evans and Lebow (1951)	Man	Femur	145,000
McElhaney (1966)	Ox	Femur	190,000 Compression
	Man	Femur	155,000 Compression
McElhaney et al.	Ox	Femur	209,000 Tension 294,000 Compression
Mather (1967)	Man	Femur	135,000 Bending
Sedlin (1965	Man	Femur	158,000 Bending
Sedlin and Hirsch (1966)	Man	Femur	159,000 Bending 63,000 Tension
Smith and Walmskey (1959)	Man	Tibia	108,000 Bending

1 from Currey (1970)

Table 1.2

Tensile Strength[1]

Author	Species	Bone	Value (kg/cm^2)
Ascenzi and Bonucci (1967)	Man	Femur	906-1,160
		Femur	1,125-1,204
Currey (1959)	Ox	Femur	1,140
Dempster and Coleman (1961)	Man	Tibia	970 along bone grain
			100 across bone grain
Evans and Bang (1967)	Man	Femur	820
		Tibia	990
		Fibula	950
Hirsch and Evans (1965)	Man	Femur	1,000 0-6 months old
McElhaney, et al. (1964)	Ox	Femur	940
Melick and Miller (1966)	Man	Tibia	1,410 less than 60 y.o.
			1,210 more than 60 y.o.
Sedlin and Hirsch (1966)	Man	Femur	890

1 from Currey (1970)

Table 1.3

Compressive Strength[1]

Author	Species	Bone	Value (kg/cm^2)
Ascenzi and Bonucci (1968)	Man	Femur	900-1,670
Bird, et al. (1968)	Ox	Femur	1,930 Longitudinal 1,550 Circumferential 1,370 Radial
Dempster and Liddicoat (1952)	Man	Femur, Tibia	1,340 Longitudinal 1,080 Circumferential 1,200 Radial
Hert, et al. (1965)	Ox	Femur	1,989 Primary Long. 2,008 Haversian Long. 1,626 Primary Circum. 1,544 Haversian Circum. 1,937 Primary Radial 1,893 Haversian Radial
	Tortoise	Humerus Femur	2,377 Primary Long
	Rabbit	Tibia	1,772 Primary Long.
	Man	Femur	2,284 Haversian Long
McElhaney (1966)	Man	Femur	1,430
	Ox	Femur	1,800
McElhaney, et al. (1964)	Ox	Femur	1,360

1 from Currey (1970)

mate tensile strength being approximately 900 - 1,100 kg/cm^2 and the ultimate compressive strength being 1,400 - 2,000 kg/cm^2. The median modulus of elasticity is approximately 1.5×10^5 kg/cm^2.

Correlation with Microstructure

The effects of varying histologies on bone mechanics have also been widely studied in static tests. Maj and Toajari (1937) investigated the correlation between breaking load and collagen fiber orientation. They found that a bone cut longitudinally took three and six times as much force to break as a bone cut tangentially or radially respectively. They concluded that the breaking strength of bone is proportional to the number of collagen fibers in the plane of the applied force. They also stated that the mechanical anisotropy of bone is dependent upon the distribution and direction of collagen fibers.

Maj (1938) studied the effects of porosity on the breaking load. He concluded that except for the distal metacarpals the variation in porosity was not responsible for the variation in the breaking load between different parts of the skeletal system. Further, he stated that the variations in strength of compact bone were probably due to the variations in density and orientation of the collagen fibers. Along similar lines Toajari (1938) concluded that the modulus of elasticity and the breaking strength of bone were directly proportional and attributable to the orientation and quality of collagen fibers.

Currey (1959) studied compact bone from ox femurs and compared tensile strength with histology. He concluded that there was a strong negative correlation between the amount of reconstruction in a bone specimen and the number of Haversian systems in it, and its tensile strength. He proffered two explanations. One was that the immature Haversian systems have large central cavities which reduce the amount of bone substance per unit volume. The other explanation was that the newly formed Haversian systems were not fully mineralized and were therefore weaker.

Ascenzi and Bonucci (1964) and Ascenzi, et al. (1966) found that the ultimate tensile strength of single osteon systems was maximal in those osteons where the majority of the collagen fibers were oriented parallel to the long axis of the test specimen.

In a series of papers Evans and Vincentelli (1969, 1974) and Vincentelli and Evans (1971) studied the correlation between the mechanical properties of human cortical bone and its histology. They found that there was a significant positive correlation between the tensile strength and tensile strain and the percent of dark osteons in polarized light (collagen bundles oriented parallel to the long axis of the osteon) and a negative correlation with the percent of light osteons in polarized light (collagen fibers oriented perpendicular to the long axis of the osteon). They claimed that there was no other significant correlation between the modulus of elasticity and the histology. They interpreted their results as being due to the predominate direction of the collagen fibers in the osteon.

Recently Saha (1974, 1976) has studied the relationship between the microstructure of bone and its dynamic strength. A highly significant ($P < .001$) negative correlation was found between the tensile impact strength and the percentage area of secondary osteons. The least squares fit of the data led to the equation

$$\sigma_u = 30.88 - .269\ X$$

where σ_u is in ksi and X is the percentage area of secondary osteons. A similar negative correlation was determined between the impact energy absorption capacity and secondary osteon area.

Influence of Bone Mineral Content

Since bone has a 65 percent inorganic mineral content it is reasonable to expect that this mineral might play an important role in determining the mechanical properties of bone. Vose and Kubula (1959) found that the modulus of elasticity and bending strength of dry bone increased with increasing ash content. In subsequent work Vose (1962) studied the breaking load from fourteen human tibias. He found a high degree of correlation between the ultimate yield loading and degree of osteoporosis ($r = -.592$, $N = 14$) and interstitial bone mineralization ($r = .857$, $N = 14$).

Currey (1969a) studied the relationship between the ash content of rabbit metatarsals and their Young's modulus, static strength, and impact strength. He found that the static strength and modulus of elasticity increased linearly with ash content. The static and impact energy

absorption capacity first increased then decreased with increasing ash content. In a subsequent paper (Currey 1969b), he proposed to explain the rapid rise in Young's modulus with ash content as being caused by an end to end fusion of apatite crystals as the matrix becomes saturated with mineral. He sites a personal communication with A. Ascenzi which suggests some electron microscopic evidence for the existence of this phenomena.

Currey (1975) in a study of bovine bone determined the amount of reconstruction and ash content in his specimens. He concluded that the variations in the mechanical properties associated with reconstruction of bone is a direct result of the varying mineral content of the bone.

Effects of Storage and Fixation

Since some time invariably elapses between the time a specimen of bone is obtained and the time its mechanical properties are measured, it is important to be aware of any effects that this elapsed period may have on the results obtained. One should also be aware of the effects that any steps that were taken to preserve the specimen might have on these results.

Frankel (1960) in a study of the breaking strength of femurs noted that there was no difference in the strength of femurs that have been frozen and those that have not been. Sedlin (1965) tested seventy-four fresh human specimens in bending, forty-three of which were tested three hours after dissection from the limb. The remaining thirty-one were

frozen at minus twenty degrees centigrade for three to four weeks and then thawed and tested. The results showed that there was no significant difference in the ultimate stress, Young's modulus, energy absorbed to failure or total deflection to failure between the two groups. He concluded that freezing to twenty degrees below zero centigrade does not alter the physical properties of bone.

The effect of drying on the mechanical properties of hard tissue was studied quite extensively by Ko (1953) who found that as the water content of bone was decreased , Young's modulus and the tensile stress at fracture also decreased. Swanson (1971) interpreted these findings as being consistent with the picture of water acting as a lubricant on the solid matrix. The results of Yokoo (1952) tend to support the above findings of Ko. Most of the subsequent work has not quantified the degree of water content in the specimens tested and are therefore felt to be not as valuable as these two earlier works.

In Evans' (1957) classic survey of the literature, he noted that the average tensile stress at fracture in embalmed bones was considerably lower than the results reported for fresh bones. He cautioned that the results were from a wide variety of sources and attempts at cross correlations were hazardous. McElhaney, et al. (1964) compared the tensile and compressive strengths of wet beef bone tested within forty hours after death and after at least fifteen hours of immersion in embalming fluid. They found that fracture stress in compression was twelve percent lower after embalming. No other significant changes with embalming were found, although other compressive and tensile properties were slightly

lower. Sedlin (1965) tested ten samples from a human bone which were studied fresh and after being immersed in ten percent formalin for three weeks. The Young's modulus showed no significant change with embalming.

Ko (1953) in his tensile tests on bone specimens stored in physiologic saline at room temperature reported no significant change in the stress-strain curve, the strain at fracture or the tensile stress at fracture as compared with fresh specimens. In reviewing this and other papers, Swanson (1971) concluded that the freshness of the sample is not crucial in mechanical testing of the mechanical properties of bone.

BONE STRUCTURE

Classification of Osseous Tissue

There are some 206 different bones of various sizes and shapes in the normal human skeleton. On an anatomical basis bone is usually classified into four main groupings: long bones, short bones, flat bones, and irregular bones. Under the heading of long bones are femur, tibia, fibula, radius, ulna, humerus, clavicle and rib. The short bones are the phalanges, metacarpals, and metatarsals. The flat bones are the bones of the skull, scapula, and ileum of the pelvis. The vertebrae, carpals, tarsals and sesamoids are irregular bones.

Each long bone is divided into several areas of interest. The shaft or diaphysis is a thick walled hollow cylinder of predominantly compact

bone with a central medullary cavity containing bone marrow and some substantia spongiosa. The epiphysis is at the end of the shaft and consists of primarily spongy bone surrounded by a thin layer of compact bone. In the immature, growing individual, the diaphysis and epiphysis are separated by an epiphysial plate where growth occurs. The intermediate area around the epiphysial plate is called the metaphysis. Except for the articulate joint areas and areas of insertion and origin of ligaments and tendons, bone is covered with a layer of specialized connective tissue called periostium. Similarly the marrow cavity is lined by a layer called the endostium. Both of these layers have osteogenic properties.

Histologically there are two classifications of bone tissue, substantial spongiosa or spongy bone and substantia compacta or compact bone. The substantial spongiosa consists of a three dimensional array of branching trabeculae or bony spicules. These trabeculae define a series of spaces which are occupied by the bone marrow. Substantia compact is grossly a solid continuous mass whose spaces can only be observed microscopically.

Histology of Bone

Bloom and Fawcett (1968) give a concise summary of bone microstructure. Compact bone is largely composed of a calcified bone matrix deposited in layers of lamellae three to seven microns thick. Within the bone substance are numerous cavities called lacunae, each of which contains an osteocyte (bone cell). Radiating from the lacunae are small passages called canaliculi that interconnect the lacunae.

The lamellae of compact bone can be classified by their architecture into several classes. The first are lamellae which are arranged around a vascular canal in bone to form a cylindrical unit called a haversian system or osteon. Between the haversian systems are irregular lamellae which are called the interstitial system, the line of demarcation between the two systems being called the cement line. The various haversian canals are interconnected by transverse cavities called Volkman's canals.

Composition of Bone

The chemical composition of bone has been the subject of extensive investigation by numerous authors. Guyton's (1971) and Bloom and Fawcett's (1968) textbooks provide some general concept of the structure of bone. However, the literature has been extensively reviewed by Herring (1964, 1968) in two articles.

Bone is composed of organic and inorganic phases. The organic phase consists of all the cellular structures and the intercellular matrix. This matrix is composed of ninety-three percent collagen, one percent mucopolysaccharide complexes and other assorted proteins. The collagen has a crystalline fibroprotein structure and periodicity of 640 angstroms. Its chemical makeup is largely amino acids with glycine, proline, and hydroxyproline making up approximately sixty percent of its total weight. Unmineralized organic matrix is composed of ninety percent water.

The inorganic phase consists of calcium, phosphate, citrate, carbonates, magnesium and hydroxyl groups. The bone crystal is often considered as a hydroxyapatite crystal with a chemical makeup of $Ca_{10}(PO_4)_6(OH)_2$ with a rod like shape and a size of 220 angstroms by 65 angstroms (Duthie and Hoaglund 1974). Substitution of the fluorine ion for the OH^- in the apatite crystal commonly occurs and is known to increase the size of the apatite crystals (Posner, et. al. 1963). Its shape is controversial but is believed to be either plate-like or pin-like. Robinson (1960) has determined that eight to nine percent of the bone matrix is composed of water.

MECHANICAL MODELS OF BONE

Elastic Properties

There have been numerous attempts to explain the physical properties of bone in terms of various mechanical models. Various models have been put forth to explain the nature of bone in terms of hydroxyapatite crystals imbedded in an organic matrix. The three elementary models of such a composite are:

a) Voigt model (upper bound)

$$E_c = E_1V_1 + E_2V_2$$

b) Reuss model (lower bound)

$$E_c = 1/(V_1/E_1 + V_2/E_2)$$

c) Hirsch model

$$1/E_c = x \frac{1}{V_1E_1 + V_2E_2} + (1 - x)(V_1/E_1 + V_2/E_2)$$

where V_1, V_2 = volume of components one and two

E_1, E_2 = Young's modulus of component one and two

E_c = Youngs' modulus of the composite

x = percent of the composite that behaves like a Voigt substance.

Katz (1971) using the results of ultrasonically determined elastic moduli of hydroxyapatite showed that the Voigt model and Reuss model can not be used to describe the composite behavior of bone. He also demonstrated that the Hashin model does not yield meaningful bounds on the experimental data. The Hashin-Strikman model was also considered by Katz, and he pointed out the models ability to establish closer bounds on the elastic behavior than the Voigt or Reuss models.

Piekarski (1973) took a similar approach to Katz. In a discursive fashion he was more willing to attribute the elastic properties exhibited by bone to the joint properties of the collagen and hydroxyapatite that it consists of. He attributed the viscoelastic properties to the flow of fluids and the viscous deformation of the gels and solutions in the bone.

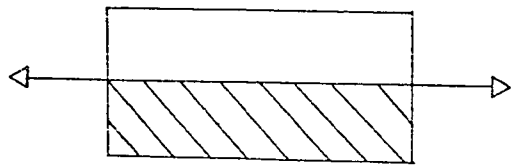

(a)

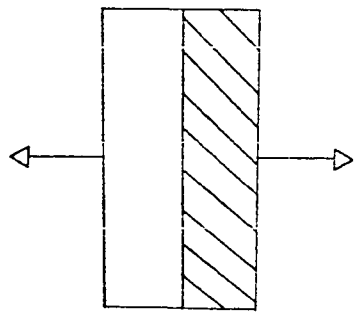

(b)

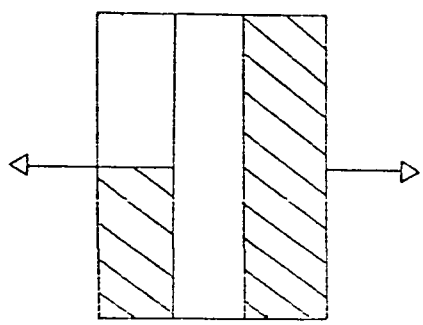

(c)

Figure 1.1 Elementary models of a composite material. (a) Voigt model, (b) Reuss model, (c) Hirsch model.

Viscoelastic Properties of Bone

It has been shown that bone exhibits the phenomena of creep and relaxation and therefore should be modeled after one of the viscoelastic models. The three important elementary viscoelastic models are the Maxwell model, the Voigt model and the standard linear model (see figure 1.2).

Sedlin (1965) attempted to explain the viscous behavior of bone in terms of the viscoelastic properties that he observed experimentally. He derived a rather complex model which was a combination of the models shown above. He claimed that his model explained most of the observed responses of bone to bending.

Lugasy and Korstoff (1969) studied the viscoelastic behavior of bovine femoral cortical bone. They concluded that the viscoelastic response of cortical bone can be represented by the superposition of collagen and hydroxyapatite crystals behaving as two distinct systems. They claimed that the collagen behaves mostly viscoelastically and the hydroxyapatite mostly elastically.

Laird and Kingsbury (1973) determined the complex viscoelastic moduli of bovine bone for a frequency range of one to sixteen kilohertz. They found that bone was a linear viscoelastic material over the range of strains that they considered. It was also felt by these investigators that the three elementary viscoelastic models did not adequately describe the behavior of bone over the frequencies they tested.

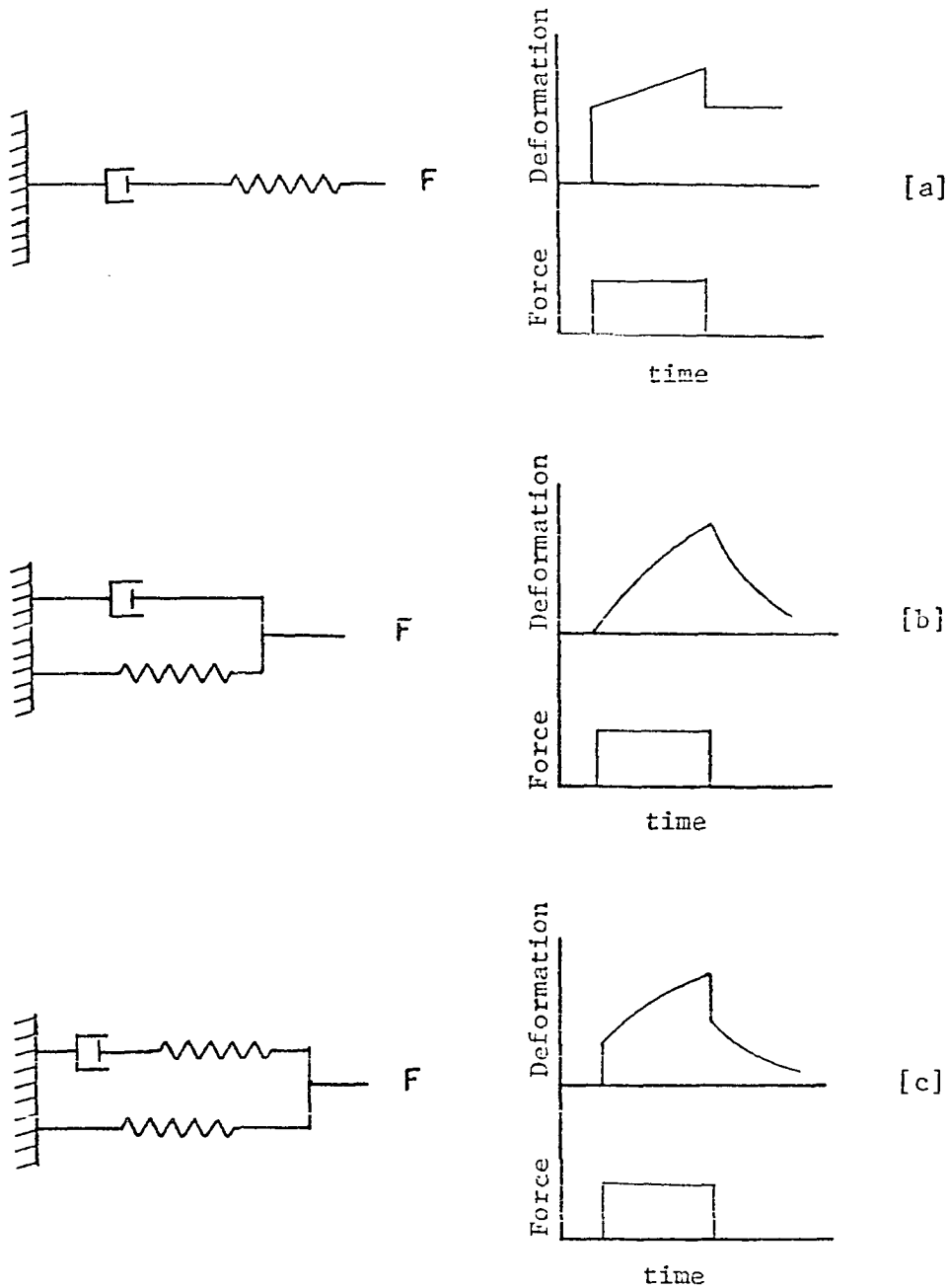

Figure 1.2 Linear Models of Viscoelasticity. [a] Maxwell model, [b] Voigt model, [c] standard linear model.

Porous Models of Bone

As mentioned above, bone tissue has numerous cavities filled with bone marrow and fluids (blood, synovial fluid, etc.) Recently, with the development of the Terzaghi-Biot theory of consolidation attempts have been made to determine the contribution of bone porosity to its physical characteristics.

Nowinski (1970) using Biot's equations derived the stress function and governing equations for a circular cylindrical bone element subject to external pressure. He considered several examples and concluded that the viscoelastic properties of the model were in agreement with the experimental findings of Sedlin (1965).

He used the porous model in another paper, (Nowinski 1971) to consider bone articulations as a system of two poroelastic bodies in contact. He considered two cases, one where the point of contact is spherical and the other when the spherical part is flat and its material rigid (e.g., a metal prosthesis). Again he concluded that the model was in agreement with the findings of Sedlin.

Nowinski and Davis (1972) treated bone as a two phase poroelastic material again using Biot's theory, and solved the problem of bending of poroelastic plates by terminal couples, pure bending of poroelastic beams of arbitrary cross-section, and pure torsion of poroelastic beams of arbitrary cross-section. The solution of the second case showed that the behavior of a poroelastic material is analogous to the three element

viscoelastic model.

In several other papers, Nowinski (1972, 1973) considered other cases of the poroelastic behavior of bone such as its effect on stress concentration around a cylindrical cavity. He found that under a constant external load the bone started to creep. This was in agreement with the results of Sedlin.

Martin and Advani (1974) treated bone as a porous material. Using Lang's (1969) coefficients along with Pope and Outwater's (1974) data, they derived a matrix which closely duplicated the observed anisotropy of diaphysial bone.

FRACTURE AND BONE REPAIR

It is well known that bone is not a static mechanical structure but responds to the mechanical stresses on it by differential growth to resist the applied stress (Justus and Luft 1970). This occurs through the selective stimulation of osteoblasts and osteoclasts. Osteoblasts are mesenchymal cells which lay down the organic matrix of bone. Osteoclasts are multinucleated cells which are responsible for bone resorption (Frost 1963).

When bone is injured or fractured, it undergoes a sequence of events to repair itself. Immediately after a bone is broken a hematoma or collection of blood forms around the fracture site. This eventually forms a fibrin clot around the fracture. The clot organizes itself and is

invaded by blood vessels. Osteoblasts and chondroblasts form within this tissue and eventually form the fracture callus. The fibrous osteoblasts lay down the new trabeculae of a fibrous bone matrix. This mineralizes after a period of time. Next, the callus is replaced by lamellar bone which is layed down along the lines of mechanical stress and strain (Frost 1973).

Various attempts have been made to explain this phenomenon. Bassett (1965) argues that areas of bone under compression (which is usually the concave side) are usually negatively charged while regions under tension (which are usually convex) are usually positively charged. It is well known that convex areas are remodeled away by osteoclast activity and concave areas are built up by osteoblasts. He argues that, therefore, bone remodeling may be due to electric phenomena. Currey (1968) claims that this model is capable of predicting the correct remodeling of a bone under a bending stress.

Recently Gjelsvik (1973a,b) developed a model that attempts to explain bone remodeling on the basis of piezoelectricity. He bases his theory on four postulates: a) The signal for surface remodeling is the piezoelectric polarization vector normal to the surface. b) The material symmetry direction of new bone deposited follows the direction of the bone on which it is growing. c) New surface bone is deposited so that no new residual stresses result. d) The material symmetry direction tries to keep aligned with the time average of the principle stress directions in the bone. He then goes on to justify these postulates from known properties of bone. In the second paper, he compares the predictions of his

model with clinical observations of the shape of longbones, bone atrophy due to disuse, shape of long bone metaphyses during growth and the correction of angular deformities in fractured long bone. He concludes that a piezoelectric model can duplicate some of the known patterns of bone remodelling.

DYNAMIC STUDIES OF BONE

The dynamic characteristics of stress wave propagation in bone such as velocity, reflection and transmission coefficients are all dependent on the physical properties of bone such as its density, elastic modulus, geometry, porosity and anisotropy. Various techniques have been used to determine the dynamic properties of bone. Three of these, namely impact testing, ultrasound and resonance studies are considered in the following discussion.

Impact Studies

Clemedson and Jonsson (1961) studied shock waves in bone created by high explosives. They showed that strong reflections occur at the boundaries between air, tissue and bone. However, they failed to quantitate the reflection and transmission coefficients. Theoretically these should be related to the difference in the acoustical impedance (= ρc) between the materials on either side of the reflective surface. Further they did not consider fracture sites or attempt to correlate their measurements

with the bone's physical or histological makeup.

McElhaney and Byars (1965) were the first to study the effect of varying velocities of impact on the mechanical response of human and bovine bone. They stated that the relationship between the ultimate strength of bone and strain rate can be reasonably well represented by an exponential curve. They further suggested a stress, strain and strain rate surface for the representation of other data. Of particular interest is their finding that a critical velocity exists for bone (at a strain rate between .1 and 1. per second) where the energy absorption capacity and maximum strain to failure are maximized.

Mather (1968) showed that the amount of energy needed to fracture the shaft of a femur varied with the rate of application of the load. He found that under impact loading, the femur had a mean energy absorbing capacity of 31.33 ft. lbs. (σ = 13.99) and under static loading conditions a capacity of 21.15 ft. lbs. (σ = 7.57) with a $p \leq .005$ and $t = 4.3$.

This is in general agreement with the qualitative conclusions drawn by Bird, et al. (1968). These workers, studying impact vs. static loading of fresh beef femur, found that there was a significant increase over static values in the compression strength of their samples over the loading range of 10^2 psi/sec to 10^5 psi/sec.

Wood (1971) studied the mechanical properties of over 120 specimens of human cranial bone in tension at strain rates from .005 to 150 per second. His findings showed that the modulus of elasticity, breaking stress and breaking strain are rate sensitive. The total energy absorbed

to failure was not rate dependent. However, he tempered these conclusions with the remark that there was a considerable amount of variation in his data that was not strain rate dependent.

Tennyson, et al. (1972) used the split Hopkinson bar technique to investigate the dynamic stress-strain characteristics of beef femur as a function of elapsed time after death. They considered a range of strain rates from ten to forty per second. A linear viscoelastic model was derived from the data from which the biomechanical properties at the time of death could be extrapolated back to.

A technique for the measurement of the dynamic properties of viable bone was established by Black and Korostoff (1973). The basis for their technique includes a rapid, sterile incision procedure which yields samples suitable for testing, a portable incubator to maintain the specimen's viability and a miniature dynamic tensile testing device with a controlled temperature and humidity environment.

Kenner, et al. (1975) used the Hopkinson bar technique to measure the dynamic elastic properties of dry compact bovine bone. They reported the velocities and strain ratios which they related to the anisotropy of the bone.

The split Hopkinson bar technique was also used by Lewis and Goldsmith (1975) to measure the dynamic properties of compact beef bone. They found that the prefracture response was viscoelastic in compression and that the fracture stress in compression increased with strain rate. They found that there was a residual plastic strain after combined torsional and

compressional loading but not with compressive loading along. A relaxation relationship that was derived from their data was given as:

$$S(t) = (3.61 - .78\ (1 - \exp - t/13/6))\ 10^6 \text{ psi}$$

t = time in microsecond

Resonance Studies

Selle and Jurist (1966) measured the resonant frequency of human ulnas using an audio generator to drive the bone. They compared these results with the degree of osteoporosis in the bone. It was concluded that the resonant frequency multiplied by the length of the bone was a monotonically increasing function of bone density and that this density could be measured within three percent by this technique compared with radiologic techniques which cannot detect osteoporosis until at least thirty percent deossification occurs (Moldawer 1963).

In a short paper, Dencker and Moberg (1968) used a 1000 Hz sound generator to diagnose the presence of soft tissue interposed between the two elements of shaft fractures in the femur and humerus. They claimed that their technique would not be useful for monitoring fracture callus but failed to elucidate their reasoning on this.

In a series of papers, Jurist (1970a,b) established the relationship between the resonant frequency (F_o), length (L) and speed of sound (c)

for a long bone as:

$$F_o L = Kc$$

where K is the proportionality constant. He then determined the ulna resonant frequency for osteoporotic, diabetic and normal patients. He found that women with symptomatic osteoporosis had a value of FL averaging forty-four percent less than that of age matched controls, and that the diabetic women had values in between the normals and osteoporotic patients. The FL values were bimodally distributed for clinically normal women over the age of forty-five years old. However, in a later note (Jurist 1972) he pointed out that the resonant frequency is critically dependent on the positioning of the ulna and apparatus, and he warned that the initial results might be due to systematic differences in the population studied.

Campbell and Jurist (1971) reported on the possible use of the measurement of mechanical impedence to study the degree of union of femoral neck fractures. They found that there were large differences in excised femurs that were either intact, status post a small wedge resection from the neck, status post complete removal of the head and after reattachment of the head. It was felt that this technique held some promise as a clinical method on monitoring such fractures.

Three models to explain the resonant frequency of a vibrating ulna were reported by Jurist and Kianian (1973). The ulna was considered as a homogeneous isotropic cylindrical tube. The first model was attached to rigid supports by hinges. In the second model the tube was attached by springs. The third was similar to the second except for the addition

of a spring mass system. All these models predicted values for the resonant frequency that were within twenty percent of the measured values.

Pugh, et al. (1973) used low audio frequencies to study the dynamic mechanical response of fresh human cancellous bone. They found that the resonant frequencies have a spectrum defined by:

$$\sigma = (h/\ell m S^2)\ n^2$$

where S is any repetitive geometric length, m is the mass of the atom that is resonating, n is any integer and h is Planck's constant. They noted that the spectrum was in agreement with a model of momentum wave modes of calcium and phosphorous atoms in the lamellae.

Doherty, et al. (1974) studied human tibial response to steady state vibration over the range of resonant frequencies. They concluded that the resonant frequency was a less sensitive indicator of osteoporotic change than either the generalized mass or stiffness.

Garner and Blackketter (1975) analyzed bone in terms of the steady state response of the forearm to harmonic excitation and put forth a finite element model of the forearm. They pointed out that Jurist only used the peak of the response curve and that more information concerning the width of the response curve should be pursued.

Ultrasound Studies

Ultrasound has been used in medicine since the 1930's and is now a common tool in medical diagnosis in cardiology, gynecology, et al. It therefore would be a natural area of investigation of non-invasive techniques to measure the mechanical properties of bone.

Anast, et al. (1958) used ultrasound in the 20 KHz range to study fracture sites. They concluded that the velocity of sound was definitely affected by the presence of a fracture, the degree of union and the maturity of the callus. They found that the wave velocity was 3481 m/sec for normal bone and 3259 m/sec for osteoporotic bone. Horn and Robinson (1965) criticized this work because there was no clear distinction between the sound delay of fresh fracture, a solid united fracture and an ununited fracture.

Rich, et al. (1966) used 3 MHz waves to show that the transit time across a bone sample was linearly related to the amount of calcium present in the bone sample in cortical bone, but not in trabecular bone. They used this data to compare calcium content of rabbit forelimb bone between predicted values from ultrasound measurements and subsequent chemical analysis of the bone samples. A very good correlation between these two methods was claimed by the authors.

The mechanical properties of healing guinea pig bones were studied by Floriani, et al. (1967) by means of 100 KHz ultrasound. They found that the velocity of ultrasonic waves were significantly decreased with

decreased healing of their experimentally produced fractures. The normal controls had a mean velocity of 3158 m/sec, completely healed bones had a mean velocity of 2968 m/sec, partly healed bones had a mean velocity of 2551 m/sec, and nonunions had a velocity of 2117 m/sec. They claimed that the velocity for the nonunions was approximately the velocity of the waves through soft tissue. However, the range of their results within each class was wide and they failed to state whether or not their results were statistically significant or not.

Recently, Brown and Mayor (1974) used a pulsed ultrasonic signal transmitted across a fracture site to study canine ulna fractures and a brass tube fracture model. They point out that a problem with the previous work that tried to differentiate the different stages of a healing fracture by means of velocity changes was that the maximum delay due to a fracture was 4.2 microseconds per cm of fracture gap. This small difference could easily be obliterated by slight fluctuations in the path length, by soft tissue changes, etc. They studied the ultrasound signal output and concluded that early callus formation could be differentiated from the later stages of healing.

Abendschein and Hyatt (1970) obtained the elastic modulus of bone by static mechanical loading tests for human femurs and tibias from cadavers and compared those results from the modulus obtained from ultrasonic testing. They obtained a relationship between the static modulus (E_s) and the dynamic, ultrasound determined modulus (E_u):

$$E_s = .134 + .7504\ E_u$$

They also concluded that the velocity is related to the density of bone and that E_s is linearly related to density.

Fresh and dried bovine bone was studied by Lang (1970) using 2.5 and 5 MHz ultrasound. In his analysis of the data he assumed that bone could be treated as a hexagonal crystal and proceeded to calculate the elastic stiffness matrix (c_{ij}, i,j = 1,6). The stress is related to the stiffness matrix by

$$\sigma_i = c_{ij}\ \varepsilon_j$$

He argued that since bone behaved as a hexagonal crystal, it could be described by only five independent stiffness coefficients which he then experimentally determined. This was done by measuring the wave propagation velocities along various axes ($v_{l_{ij}}$), and then by using the relationship:

$$c_{11} = \rho\ (v_{l_{11}})^2\ , \text{ etc.}$$

he calculated the Young's modulus as a function of the angle from the bone axis. This was found to be extremely anisotropic, while the shear modului were isotropic.

Grenoble, et al. (1972) used 35 and 30 MHz ultrasound to determine the pressure dependence of Poisson's ratio, Young's modulus, bulk modulus and shear modulus in hydroxyapatite, fluorapatite, chlorapatite, human bone and other hard tissue. They showed that the mineral portion of the hard tissues measured behaved differently than the hydroxyapatite. Their results differ from Lang's. However, their experiments were done at high

pressure on isotropic porous powders while Langs were obtained at atmospheric pressure on porous oriented specimens.

Theoretical Studies

There are relatively few studies attempting to describe the dynamic response of bone. Some of these are presented here.

Nowinski and Davis (1971), using Biot's theory of poroelasticity treated bone as a porous solid circular cylinder. It should be pointed out that long bones have a central marrow cavity. Therefore, their assumption of a solid cylinder is not a very realistic model for long bones. The wave velocities for bone were calculated to be 3.6×10^3 and 2.5×10^3 m/sec. These results bounded the value of 3.07×10^3 m/sec reported by McElhaney and Byars (1967). However, Pelker and Saha (1975a) pointed out several errors in their treatment of the problem.

Vayo and Ghista (1971) considered the problem of the two layered bone and the special case of compact bone by solving the elastic wave equations in terms of Bessel functions using a multilayered cylinder as a model. They then used Lang's (1970) coefficients to calculate the wave velocity for compact bone in the short wavelength limit. They bypassed the intermediate wavelength region as being too complex for analytic solution. They found three values for the wave velocity 3380 m/sec, 1790 m/sec and 1420 m/sec corresponding to three different wavenumbers, $q = 1.86$, 3.52 and 4.42 cm^{-1} respectively.

Burtula and Pope (1973) constructed a finite element model for a wave propagation in bone. Using the elastic moduli of bone (Pope 1974) and moduli for partially healed fractures and fractures with bony union (Abendschen and Hyatt 1970) they calculated the wave velocity for bone. They reported a wave velocity of 1080 ft/sec for intact bone and 1030 ft/sec for freshly fractured bone. They also measured the in vivo wave velocity of a human tibia using a wave generated by a hammer and a tuning fork. They claimed a measured velocity of approximately 100 ft/sec. Since this was for a bending wave, it cannot be compared with the results of others who measured the longitudinal wave velocity.

Lewis (1975) recently modeled bone fractures as two elastic rods joined together by a compliant section between them. He presented the resonant frequencies and mode shapes for a range of stiffness coefficients of these compliant elements. A comparison of these theoretical predictions were made with a series of experiments with epoxy and urethane rubber elements. He noted that any attempts at monitoring fracture healing by accelerometer output in a vibrating specimen will be very dependent on the ability to keep the position of the inputs and outputs constant.

Summary

From the survey of the field presented above, it can readily be seen that the study of the dynamic response of osseous tissue is of active interest to many researchers. It can be stated that bone is now assumed to be stronger in the dynamic situation than in the static case. The study of the resonant response of bone has been studied extensively, especially

by Jurist. However, the problem with this technique remains its extreme sensitivity to the position of the driver and detector. The use of ultrasound has also gained certain degree of popularity. However, attempts at measuring fracture healing by velocity changes through the fracture are hindered by the small time delay over the callus site. Finally, there is an enormous paucity of information regarding the transmission and reflection coefficients in bone in general and in a healing fracture in specific.

Chapter II

LONGITUDINAL WAVE PROPAGATION IN BONE

INTRODUCTION

As has been discussed previously, there have been several attempts at measuring the dynamic properties of bone. However, very little has been done with respect to the measurement of longitudinal stress waves in bone. The tripart purpose of this set of experiments is to first test various techniques of measuring stress waves in bone with the aim of finding methods that might be applicable to in vivo studies. Next it is hoped that some of the basic characteristics of stress wave propagation in normal bone will be established. Finally, the characteristic changes of a stress wave propagating through a simulated fracture were investigated.

It is hoped that once the basic properties of the dynamic response of bone is fully understood then this physical property can be used to extract useful clinical information about the skeletal system of patients.

In pursuit of this goal compressive impact tests were performed on fresh and embalmed, wet and dry human long bones. The stress wave characteristics were monitored by means of strain gages and a magnetic velocitometer developed for this work. When these tests were finished, a series of simulated fractures were produced in the test specimens and the tests repeated to observe any changes in the characteristics of the transmitted wave.

MATERIAL AND METHODS

Bone Specimens

All bone specimens were obtained from human cadavers obtained from the Anatomy Department of the Yale University School of Medicine. The test material consisted of twelve human long bones (tibias, femurs and humeri), six fresh and six embalmed. All soft tissue (muscle, tendon, etc.) was carefully dissected away from the specimens and the bones disarticulated. There was no known history of bone disease in any of the cadavers from which the bones were obtained.

All specimens were kept frozen at minus twenty degrees centigrade until needed for testing. At that time they were thawed to room temperature. Previous investigators have shown that this freezing and subsequent thawing does not significantly alter the mechanical properties of bone (Sedlin 1965).

While being thawed, all bones were kept moist. This was accomplished by wrapping the specimens in gauze and saturating the gauze with a solution of Ringer's lactate solution (this consists of water with 103 MEq/L NaCl, 27 Meq/L Na lactate, 4 MEq/L KCl, and 4 MEq/L $CaCl_2$). Ko (1953) has shown that specimens stored at room temperature in physiologic saline undergo no change in their stress strain curve. The gauze and bone were then wrapped in plastic to insure a constant moisture environment.

Measurement Techniques - Strain Gages

The use of strain gages to measure the biomechanical properties of bone have been described by several authors (Roberts 1965, Lanyon 1871, 1973, Cochran 1972, 1974, Hobbobl 1972, Barnes and Pinder 1974, 1975 and Salmons 1975). For the studies done here it was decided after several preliminary tests, to use semiconductor strain gages instead of the conventional wire resistence strain gages. The high gage factor of the semiconductor provided a signal approximately one order of magnitude greater than the signal from wire resistance gages. This provided a maximum signal to noise ratio. BLH SR-4 semiconductor strain gages were chosen for this purpose. The gages were bonded to the bone in the standard fashion using "Eastman 910" adhesive. Gages were mounted on the proximal and distal segments of each bone specimen. The gages and all electrical leads to the gages were coated with a layer of "BLH gagecoat waterproofing" to allow testing of the specimens in the wet condition. A set of Wheatstone bridges was constructed for balancing the strain gages. The output

from the bridge circuit was fed into a set of Tektronics oscilloscope amplifiers. The output from these was fed into a Tektronics dual trace storage oscilloscope from which the measurements were recorded (see Fig. 2.1).

Measurement Techniques - Magnetic Velocitometer

Ripperger and Yeakley (1963) developed a technique (described below) for measuring the particle velocities in a rod. This was used by Effron and Malvern (1969 to study plastic waves in aluminum bars. The method described here is a adaptation of their technique which consisted of measuring the voltage generated in a loop of wire coiled around the specimen and placed in a magnetic field. The voltage generated was a result of an impact at one end of the specimen causing the wire to move.

The technique is based on Faraday's principle that a moving wire in a magnetic field will generate a voltage across the ends of the wire, which is proportional to the magnetic field, the length of the wire in the magnetic field and the velocity of the wire. This can be simply expressed as:

$$E = \vec{B} \cdot \vec{L} \times \vec{V}$$

where E = the voltage across the wire

$\vec{B}$ = the magnetic field vector

$\vec{L}$ = the length vector of the wire

$\vec{V}$ = the velocity of the wire

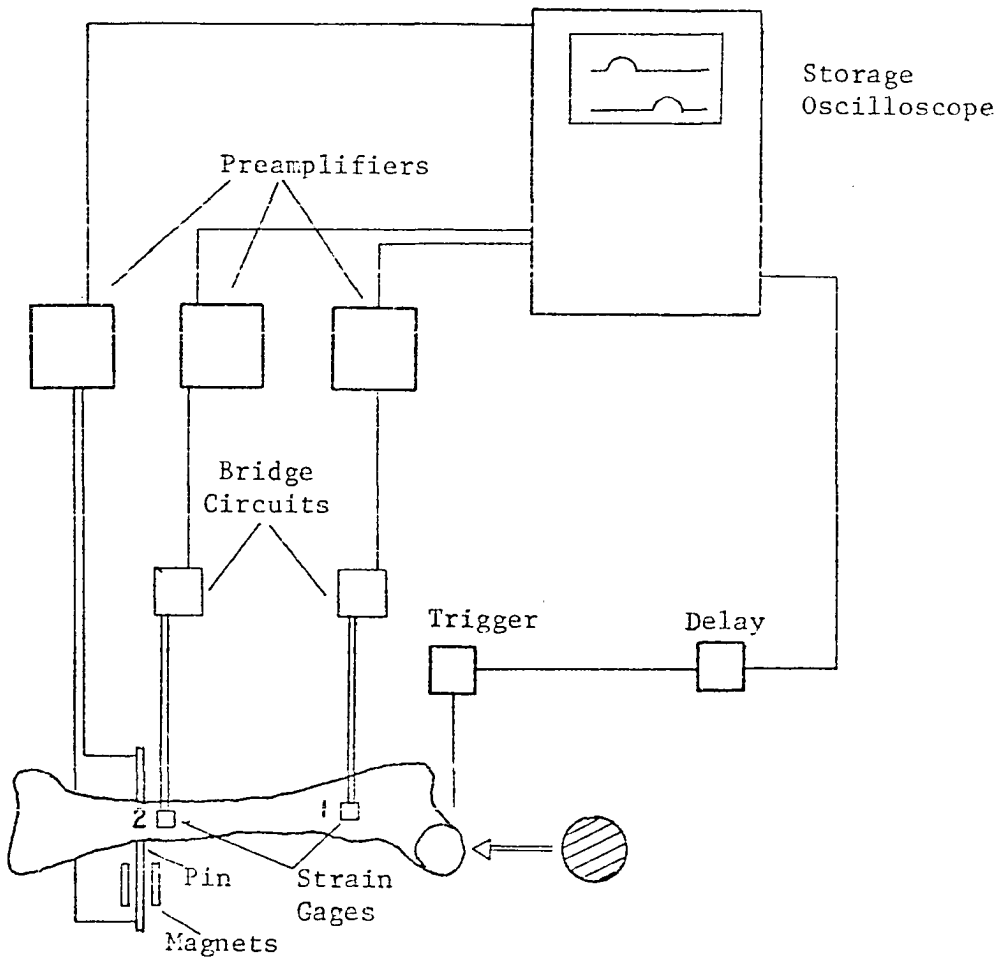

Fig. 2.1 Block diagram of experimental setup

However, in this work a threaded skeletal traction pin was used in place of the wire coil that was used by previous experimenters. This nonmagnetic, electrically conducting pin was placed through the bone at a site corresponding to the distal strain gage station. The bone with the pin in it was then placed in the magnetic field provided by two permanent magnets.

A special alignment rig was designed to ensure the constant and reproducible placement of the pin in the center of the magnetic field. Another rig was constructed to enable one to align the lead wires so that they were perpendicular to the magnetic field. This is important since if the wires were not perpendicular to the field then the $\vec{B} \cdot \vec{L}$ (= $|\vec{B}||\vec{L}|$ cos 6) contribution to the output from the lead wires would not be zero. Therefore, any slight movement of these lead wires would contribute to the measured output from the skeletal traction pins.

As in the strain gage measurements, the lead wires were connected to Tektronics oscilloscope amplifiers and the amplified signal was stored on a Tektronics dual trace storage oscilloscope from which the measurements were recorded (see Fig. 2.1). Fig. 2.2 shows a typical output from this technique and the strain gage technique.

Impulse Production

The compressive stress pulse was generated by the impact of a ½ inch diameter steel ball bearing on the proximal end of the test specimen from

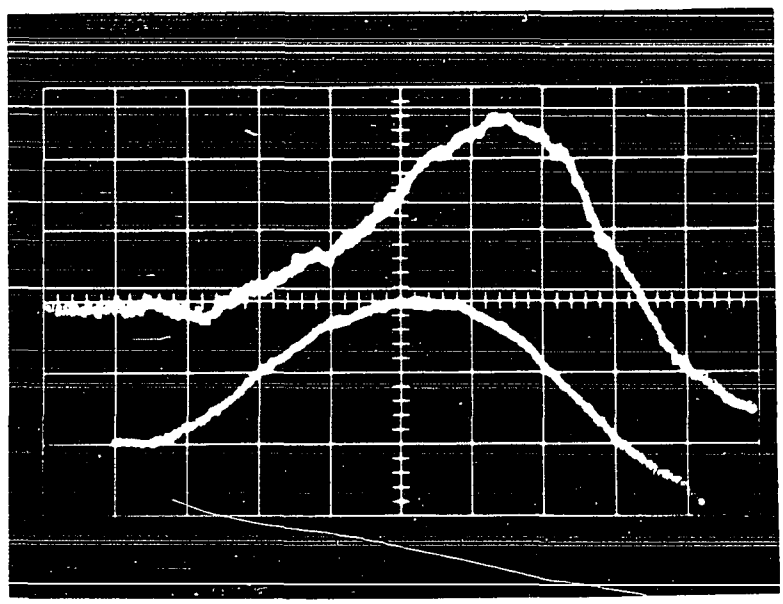

Figure 2.2 Typical output for strain gage at station two (bottom curve) and skeletal traction pin detector (top curve). The horizontal scale is 20μsec per major division.

a constant height of fifteen cm. The size of the ball bearing and the height of the impact were determined by a compromise of several factors to optimize the pulse width, maximize the signal to noise ratio and to ensure minimal damage to the test specimen. By varying the height of the impact and thus varying the energy of the impact, the measured wave energy was shown to correlate linearly with the energy of the impact for the range of impact energies considered here.

Oscilloscope Triggering

A triggering circuit was constructed to establish the time of the initial impact. The oscilloscope used to record the strain gage and pin outputs was triggered by the closing of an electric circuit upon the contact of the ball bearing used for the impact with the bone. The timing of this triggering pulse could be varied by means of a delaying circuit. This allowed one to optimally position the trace of the pulse on the oscilloscope screen.

Calibration of Amplifiers

The output from the amplifiers were measured for a series of known input voltages surrounding the expected output from the strain gages and the pin detector. Both oscilloscope amplifiers were found to be linear in the region that they were to be used. Each one provided a voltage amplification of 228.

Calibration of Strain Gages

Each Wheatstone bridge was calibrated prior to each series of tests. This was accomplished by means of a series of shunt resistances across each strain gage. This simulated the change in resistance of the gage that would occur with an actual strain. As long as the shunt resistance (R_s) is much smaller than the gage resistance (R_g), i.e. one is operating in the linear region of the bridge circuit, then the simulated shunt strain (ε_{sim}) can be expressed as:

$$\varepsilon_{sim} = R_g/(R_s F)$$

where F = the gage factor.

Then the actual experimental stress can be expressed in terms of the measured voltage.

$$\varepsilon_{exp} = \varepsilon_{sim} \frac{E_{exp}}{E_{sim}} = \frac{R_g}{F} \frac{1}{R_s E_{sim}} E_{exp}$$

where E_{exp} = voltage output during actual testing

E_{sim} = voltage output during calibration shunting

Thus,

$$\varepsilon_{exp} = E_{exp} \alpha$$

where $$\alpha = R_g/(F R_s E_{sim})$$

A number of values for R_s were used to obtain a series of values for $R_s E_{sim}$. The mean of these values was then taken to give a final value

of α that was used to calculate the strains. This calibration procedure was carried out on each of the strain gages used.

Fracture Techniques

After studying the wave propagation characteristics for intact bone, simulated partial fractures were produced in the bone samples. This was done by carefully making serial circular cuts into the bone cortex. A narrow file was used for this purpose in order to minimize any destructive temperature changes that might be produced by high speed power equipment. The width of the cut was approximately 2 mm. The depth of the simulated fracture was carefully measured with a machinist's depth gage. The compressive impulse tests were then repeated and then a deeper cut was made. This was done at approximately .075 cm intervals until the bone was completely fractured.

Porosity

Since attempts are being made by several authors (Nowinski and Davis 1971 and Pelker and Saha 1975) to establish a model of bone that encompasses the porosity of bone, it would be useful to correlate the findings of this work with the specimens' porosity. The standard technique for measuring bone porosity was described by Evans (1958) and Evans and Bang (1966). It consists of taking photomicrographs of cut sections of bone.

From these photographs the areas of the pores and the area of the solid bone are measured.

In this study a sample of bone was taken from the area surrounding the site where the specimen was fractured. This specimen was then embedded in an epoxy resin (DTA activator added to epon 815). The specimen was then polished, coated with India ink and then repolished. This allowed for maximal contrast between the pores and bone sample. A combination of transmitted and reflected light photomicrographs were taken of these samples. The areas corresponding to the pores (haversian canals, vessels, etc.) were maximally stained using this system (see Fig. 2.3). The ratio of the pore area to the total specimen area gives a measure of the porosity of the bone specimen.

$$\text{Porosity} = A_1/A_0$$

where A_o = total specimen area

A_1 = area of specimen stained with India ink

This measurement was accomplished using an Amtech Inc. Image Analyser which functions as an electronic planimeter by intensity analyzing the light transmitted through the photographic negative. A grid was made with an area corresponding to a pore area of 20 percent (= porosity). The area as measured by the electronic planimeter was 20.1 percent. Thus, it can be seen that this method is quite accurate for porosity measurements. Further it is much less time consuming than the conventional method for measuring porosity described above.

Figure 2.3 Typical photomicrograph of bone specimen used to make porosity measurements, stained as specified in text.

Bone Mineral Content

An approximate measurement of the bone mineral density by means of radiologic techniques has been described by Keane, et al. (1959), Meema, et al. (1964) and Doyle (1968). Roentgenographs of each bone specimen were made along with an aluminum wedge with steps from 1 mm to 1.5 cm. The radiographs were taken at 100 milliamps, 48 kilovolts for 1/30 second at a distance of 40 inches (see Fig. 2.4). Each radiograph was scanned five times with a Macbeth TD 102 photodensitometer whose output was recorded on a chart recorder. The scanning window was approximately 1 mm. The first scan was of the aluminum step wedge. Then the x-ray of the bone was scanned at four different sites, two on each side of the fracture site. Thus, the radiographic bone density could be directly compared to the aluminum calibration wedge on each roentgenograph. Doyle stated in the above article that 1 mm of aluminum corresponds to 155 mgm/cm^2 of bone ash. Thus, the mineral content of each bone specimen was estimated. A typical aluminum wedge calibration curve is shown in Fig. 2.5

RESULTS

Intact Wet Bone

The strains in a whole femur due to a longitudinal impact of a ½ inch diameter steel ball falling from a height of fifteen cm were of the

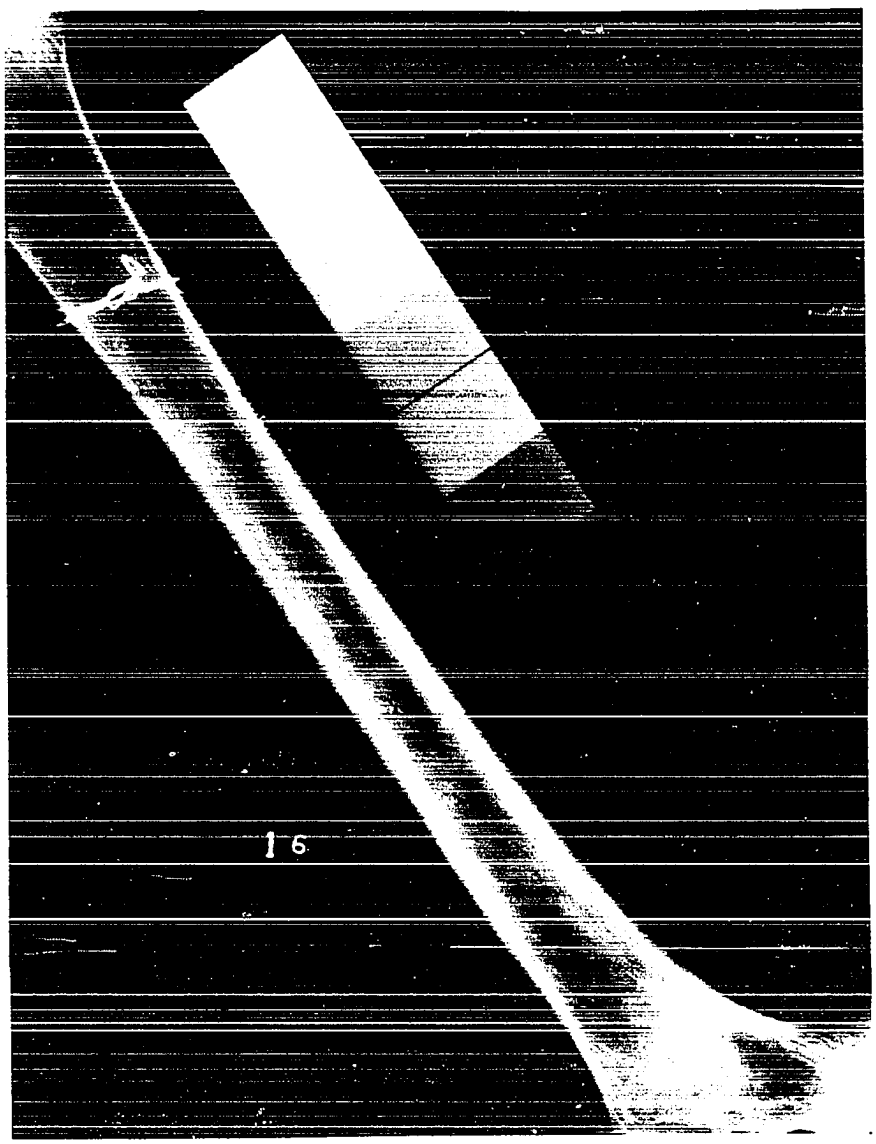

Figure 2.4 Typical radiograph of intact bone specimen and aluminum calibration wedge.

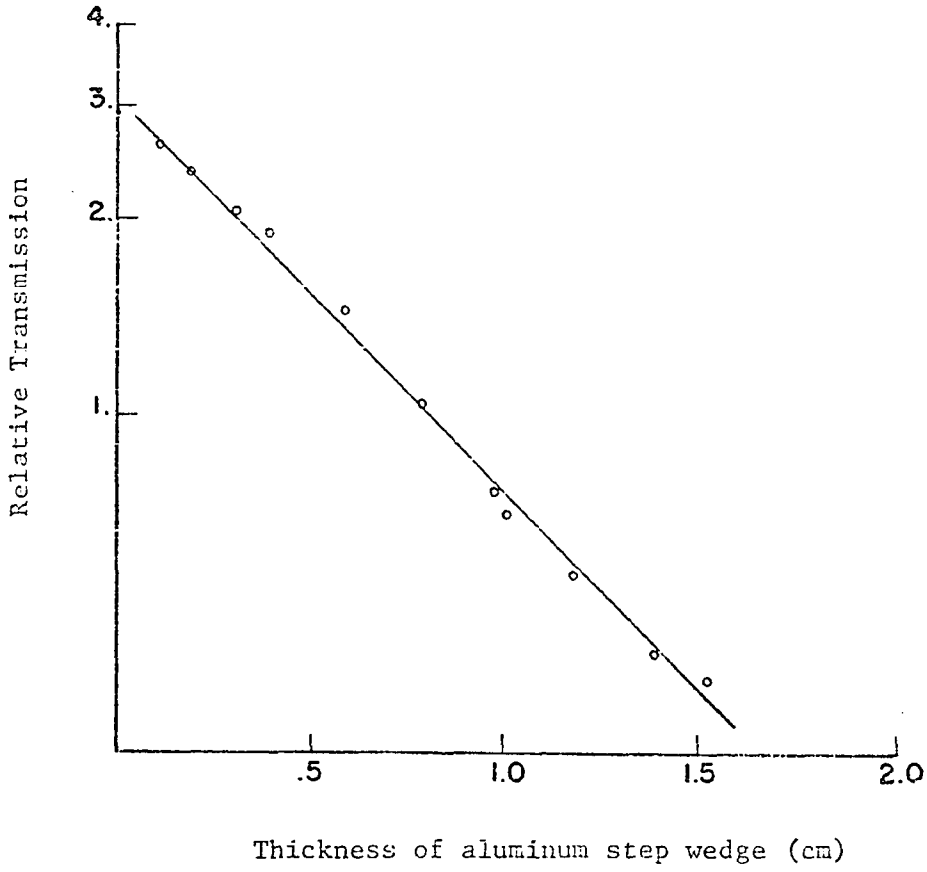

Figure 2.5 Typical calibration curve for aluminum step wedge.

order of 5×10^{-5}. Figure 2.6 shows a typical strain output. The initial compressive pulse is shown as the positive portion of the curve, and the tensile pulse due to reflection off the distal end of the bone is shown as the trailing negative portion.

The viscoelastic damping coefficient was calculated for the fresh, wet and dry specimens by using:

$$\varepsilon = \varepsilon_o \exp(-\alpha x) \qquad \text{Kolsky (1963)}$$

$$\alpha = -1/x \, (\ln \varepsilon/\varepsilon_o)$$

where ε_o = the strain measured at the proximal strain gage station

ε = the strain measured at the distal strain gage station

x = the path length between the strain gages

The results of this calculation are given below for the twelve specimens.

Table 2.1

Experimental Damping Coefficients (2)

	cm^{-1}	
fresh bone	.023	± .030
embalmed wet bone	.058	± .035

The velocities of stress wave propagation were determined by measuring the time elapsed between the arrival of the pulse peak between the two strain gage stations. This value was then divided into the distance between the two stations to give the velocity, i.e.

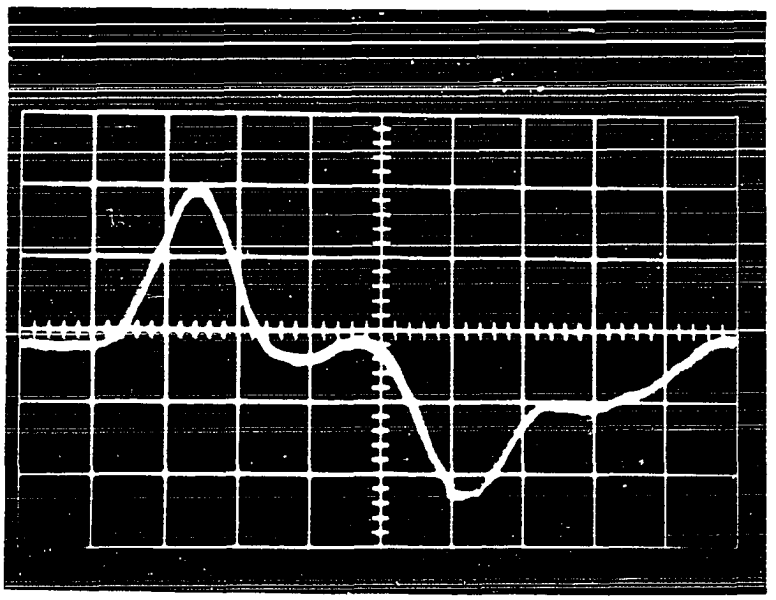

Figure 2.6 Typical output of strain gage. The positive portion of the curve represents the initial compressive wave. The trailing negative portion represents the reflection of this wave off the distal boundary of the bone. The horizontal scale is 50 μsec per major division, the vertical scale is approximately 1.2×10^{-5} per major division.

$$v = \ell/t$$

where v = velocity of the pulse

ℓ = distance between strain gage stations

t = measured time elapsed between arrival of pulse peak at each station.

The velocities determined for fresh, wet and dry bone are listed below for the twelve bone specimens.

Table 2.2

Experimental Velocity Measurements

	velocity (m/sec)	
fresh bone	3377	± 370
embalmed wet bone	3228	± 110

The broadening of the wave pulse was determined by measuring the pulse width at half maximum at both strain gage stations. The "broadening factor" was simply taken to be the ratio of the distal width to the proximal width, i.e.

$$\text{Broadening} = (\tau_{1/2})_2 \; / \; (\tau_{1/2})_1$$

where $(\tau_{1/2})_1$ = pulse width at half maximum at the proximal strain gage station

$(\tau_{1/2})_2$ = pulse width at half maximum at the distal strain gage station.

The results from this series of measurements can be found in the table below for the twelve bone specimens.

Table 2.3

Experimental Broadening Coefficient

fresh bone	1.07	± .12
embalmed wet bone	.96	± .07

The effects of drying were studied on a subset of embalmed bones which were allowed to air dry for a minimum of two weeks before remeasuring. The results from this set of measurements on four specimens are reported below.

Table 2.4

Effects of Drying on Embalmed Bone

Damping Coefficient	.083	± .013	.069	± .009
Velocity	3232	± 131	3246	± 235
Broadening Coefficient	.99	± .03	1.0	± .05

Simulated Fracture Healing

After the above intact tests were completed, serial cuts were made into the bone samples to simulate a fracture at a stage of healing related to the remaining thickness of cortex. Figure 2.7 shows typical

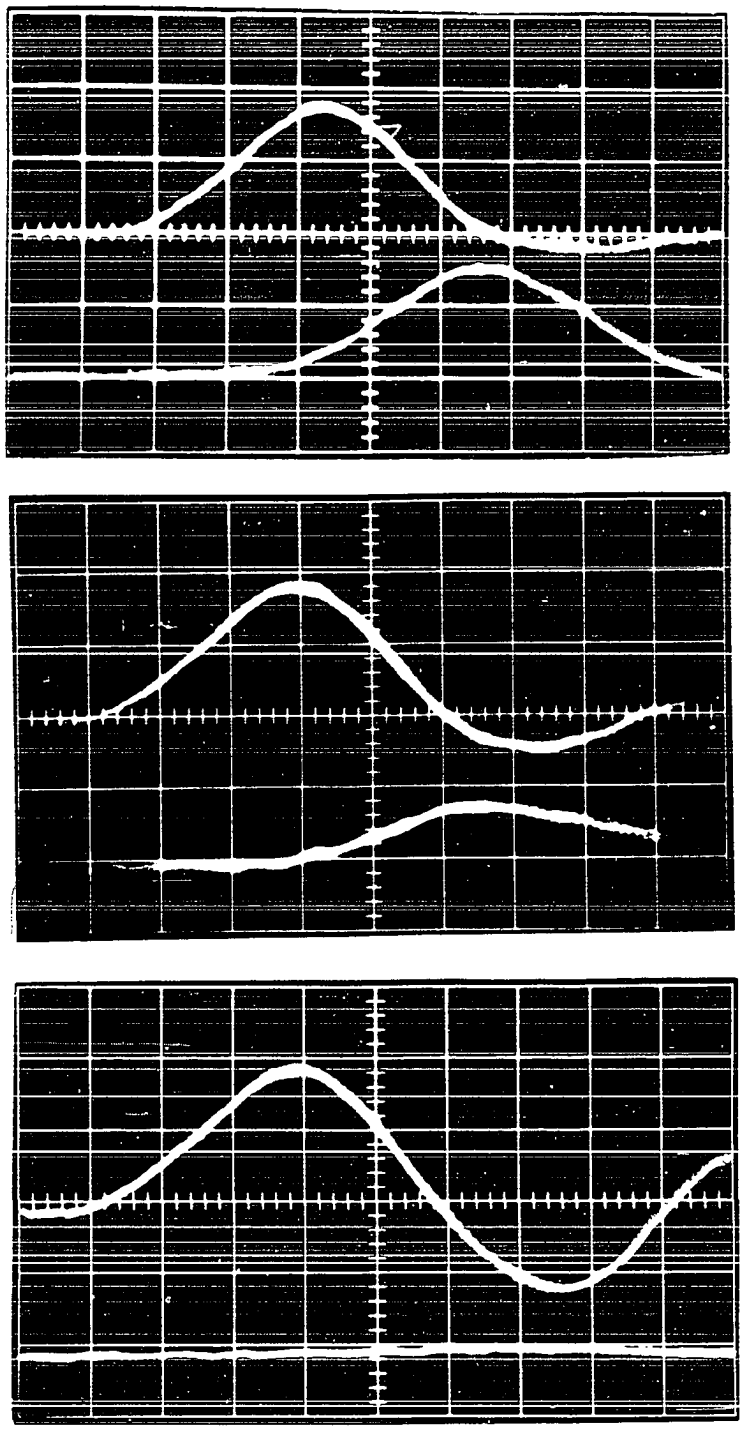

Figure 2.7 This set of outputs represents a typical sequence of wave changes as a bone is serially fractured. The top curve is from an intact bone, the middle one from the same bone after a .32 cm cut and the bottom one from the same bone after it has been completely sectioned. The horizontal scale is 20 μsec per major division.

pulses for a series of progressively deeper cuts into the bone cortex (i.e. corresponding to an early stage of healing).

All of the fracture plots described below were plotted against a normalized cross sectional area. This normalized area was taken as the ratio of the cross sectional area left after a fracture cut (A) to the original cross sectional area (A_o). The bone was treated as a hollow circular cylinder whose inner and outer radii (b and a respectively) were taken as an average of their values along the major and minor axis of the cross section. The areas computed from these values were found to be within 8 percent of the areas obtained by planimeter measurement of a random sampling of bone specimens. Table 2.5 shows this in detail and gives geometric and physical data on each specimen. Further, each curve shown below was arrived at by means of a least squares fit of the data points to either the parabolic function $y = A + Bx + C x^2$ or the linear function $y = A + Bx$, using a HP9805A calculator. The coefficient of determination (r^2) and the significance level were also determined.

The transmission coefficients were calculated for the original intact specimens by taking the ratios of the strains at station one and two, i.e.

$$T_o = \varepsilon_2/\varepsilon_1$$

where T_o = the original transmission coefficient

ε_1 = strain at station 1

ε_2 = strain at station 2

Table 2.5

Geometric and Physical Properties of Specimens

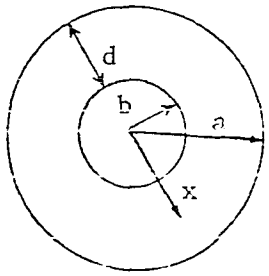

$A_0 = \pi(a^2 - b^2)$

$A = \pi(x^2 - b^2)$

Specimen	(cm)	(cm)	(cm)	(cm)	Equiv. Density (g/cc)	Poro-sity (%)
1	1.44	.96	.48	3.62	1.02	11
2	1.86	1.11	.75	7.00	1.25	14
3	1.55	.95	.60	4.71	1.28	3.4
4	1.95	1.43	.52	5.52	1.10	4.3
5	2.70	2.06	.64	9.57	1.10	9.3
6	1.78	1.11	.67	6.08	1.06	6.7
7	1.37	.85	.52	3.63	.99	25.7
8	1.35	.83	.52	3.56	1.04	14.2
9	.87	.55	.32	1.43	1.30	4.3
10	.91	.47	.44	1.91	1.57	13.3
11	1.07	.63	.44	2.35	.97	14.1
12	1.13	.77	.36	2.15	1.33	6.9

Also, the uncorrected transmission coefficients for each fracture depth were calculated by taking the ratios of the strain at the two stations, i.e.

$$T_{fx} = (\varepsilon_2/\varepsilon_1)_{fx}$$

where T_{fx} = the uncorrected transmission coefficient

Finally, by taking the ratio of these two coefficients the transmission coefficient corrected for the viscoelastic damping in each specimen is arrived at.

$$T = T_{fx}/T_o$$

Thus, we have the transmission coefficient due to the fracture alone. The results of the calculations are plotted against the normalized area in Figure 2.8. The solid curve is the least squares fit of the data (with the end points of a normalized area of 0 and 1 excluded) below a normalized area of .6 and the dash-dot curve below .8. The resultant linear regression curves are respectively

$$T = .46 + .95\ A/A_o \qquad (r^2 = .4296,\ S = .001)$$

$$T = .52 + .66\ A/A_o \qquad (r^2 = .2662,\ S = .001)$$

A fit of all data points to a parabolic function resulted in the regression relation

$$T = .17 + 2.55\ A/A_o - 1.75\ (A/A_o)^2 \qquad (r^2 = .78,\ S = .001)$$

Similar to the above manipulations a ratio of the broadening coefficients was calculated to give an estimate of the dispersion caused by the

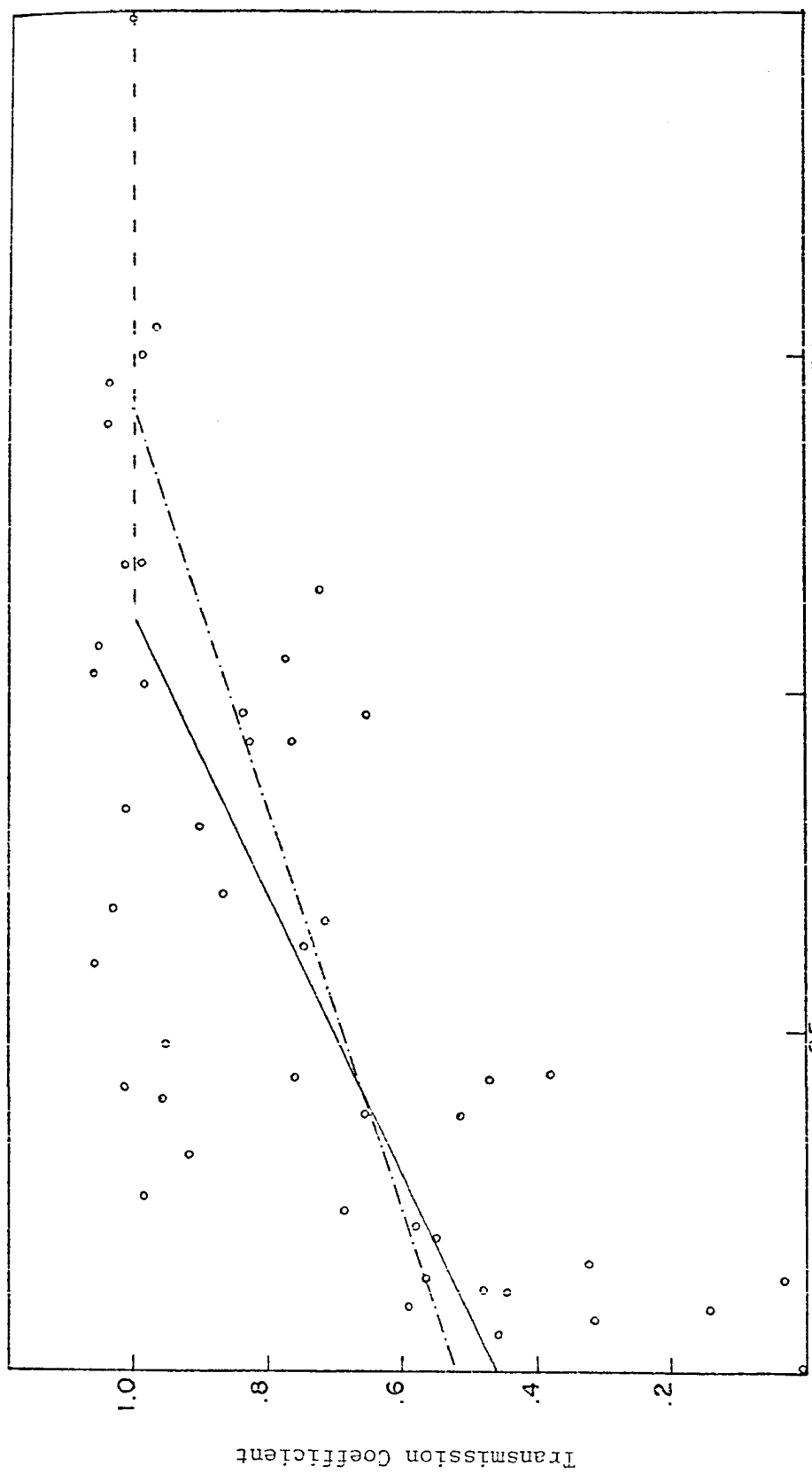

Figure 2.8 Experimental Transmission Coefficient vs. Normalized Area.

fracture. This can be summarized as:

$$D = B_{fx}/B_o$$

where D = the "dispersion coefficient"

B_{fx} = broadening due to the fracture

B_o = original broadening coefficient

However since $B_o \cong 1.0$ we have

$$D \cong B_{fx}$$

This set of data for dispersion coefficients was plotted in Figure 2.9 against a normalized area. The solid curve is the least squares fit of the data (with the end points of a normalized area of 0 and 1 excluded) below a normalized area of .6 and the dash dot curve below .8. The resultant linear regression curves are respectively

$$D = 1.30 - .54\ A/A_o \qquad (r^2 = .3333,\ S = .001)$$

$$D = 1.29 - .49\ A/A_o \qquad (r^2 = .3847,\ S = .001)$$

A fit of all data points to a parabolic function resulted in the regression relation

$$D = 1.35 - .98\ A/A_o + .64\ (A/A_o)^2 \qquad (r^2 = .49,\ S = .001)$$

The time delay of the arrival of the compression pulse due to the presence of the increasing fracture depth was calculated. This was done by subtracting the transit time for the pulse to travel between the two strain gage stations for the simulated healing (partially fractured) bone

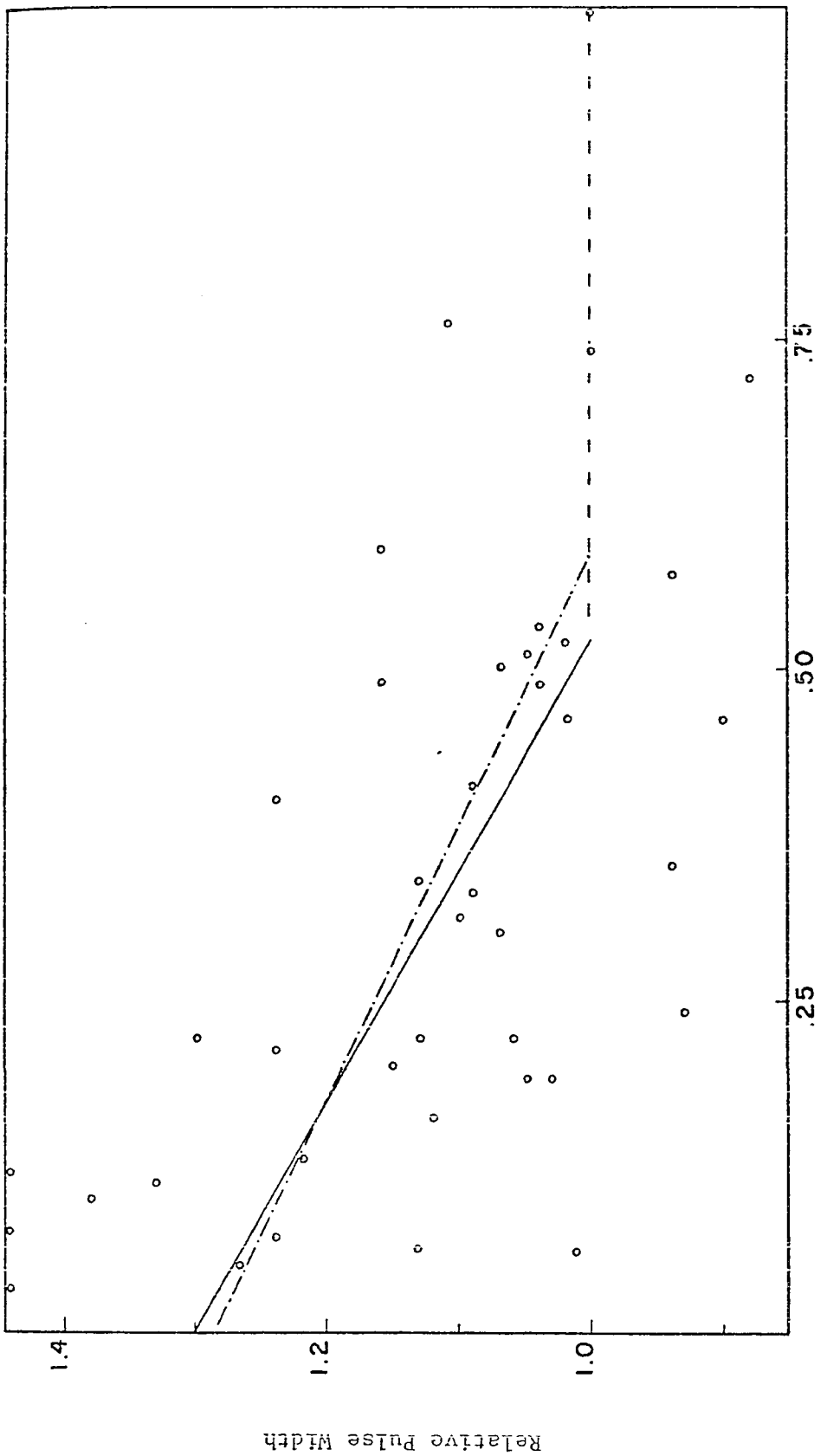

Figure 2.9 Experimental Pulse Width vs. Normalized Area.

from the original transit time for unfractured bone.

$$\Delta = \Delta_{fx} - \Delta_o$$

where Δ_o = transit time in unfractured bone

Δ_{fx} = transit time in fractured bone

These results were plotted in Figure 2.10 against the normalized area. The solid curve is the least squares fit of the data (with the end points of a normalized area of 0 and 1 excluded) below a normalized area of .6 and the dash dot curve below .8. The resultant linear regression curves are respectively

$$\Delta = 40.24 - 75.94\ A/A_o \qquad (r^2 = .5301,\ S = .001)$$

$$\Delta = 37.12 - 60.81\ A/A_o \qquad (r^2 = .5456,\ S = .001)$$

A fit of all data points to a parabolic function resulted in the regression relation

$$\Delta = 45.12 - 124.38\ A/A_o + 79.62\ (A/A_o) \qquad (r^2 = .71,\ S = .001)$$

Skeletal Traction Pin Detector

The results from the skeletal traction pin detector were recalculated as a ratio of the pulse height after a given fracture to the original pulse height before fracture. This gives a transmission coefficient for the pin detector due to the fracture and corrected for any damping.

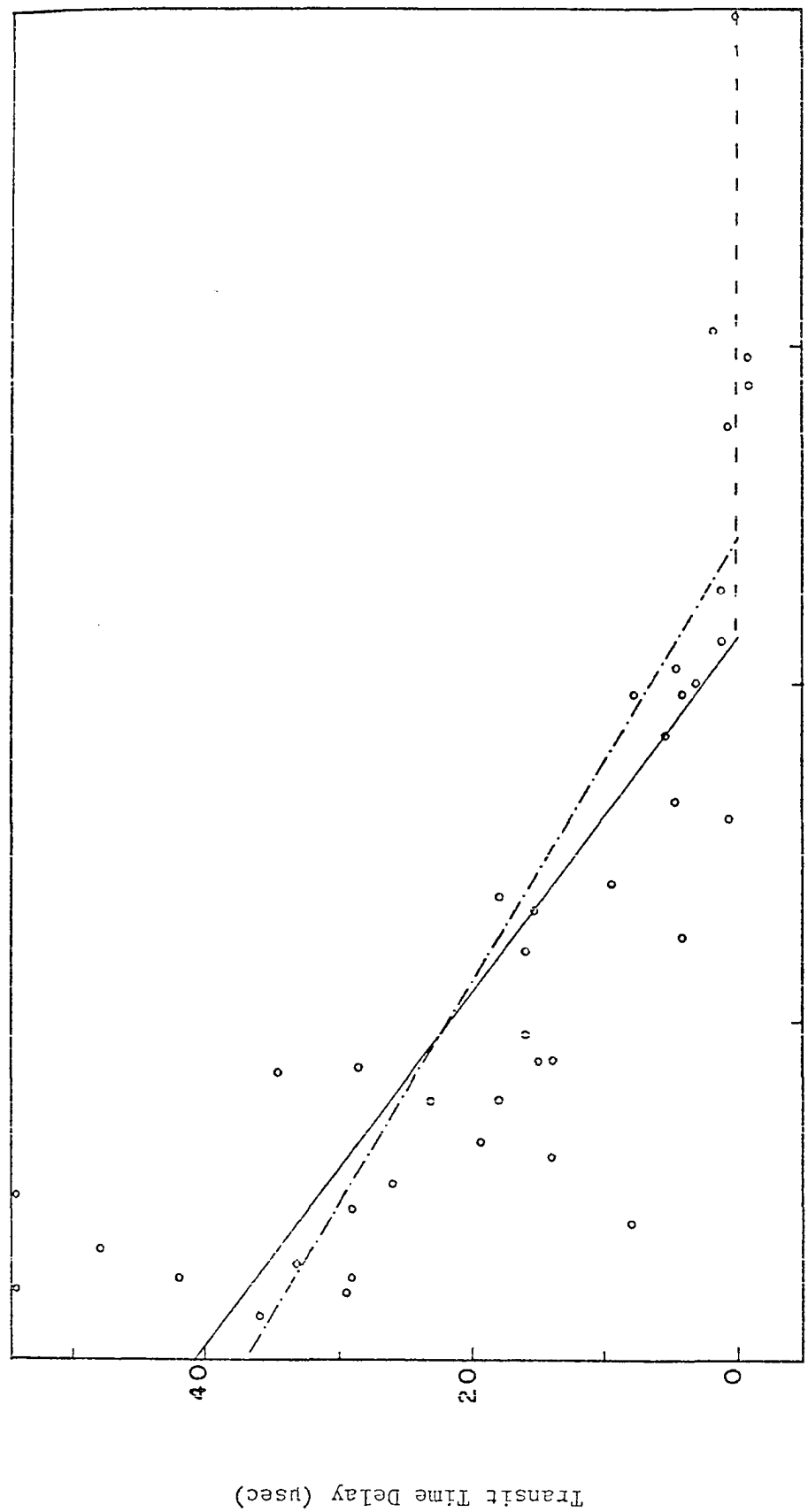

Figure 2.10 Experimental Transit Time Delay vs. Normalized Area.

$$T_{pin} = P_{pin}/P_{pin_o}$$

where P_{pin_o} = pulse height of the pin detector before fracture

P_{pin} = pulse height of the pin detector after fracture

The results of this calculation are plotted in Figure 2.11. The solid curve is the least squares fit of the data (with the end points of a normalized area of 0 and 1 excluded) below a normalized area of .6 and the dash-dot curve below .8. The resultant linear regression curves are respectively

$$T_{pin} = .65 + .66\ A/A_o \qquad (r^2 = .3310,\ S = .001)$$

$$T_{pin} = .33 + 1.32\ A/A_o \qquad (r^2 = .5459,\ S = .001)$$

A fit of all data points to a parabolic function resulted in the regression relation

$$T_{pin} = .25 + 2.64\ A/A_o - 1.94\ (A/A_o)^2 \qquad (r^2 = .70,\ S = .001)$$

Table 2.6 lists the coefficients of determination for the linear and parabolic cross correlations of the experimental variables.

DISCUSSION

Intact Bone

It can be seen from Table 2.1 that the measured viscoelastic damping coefficients do not appear to be affected to any statistically significant

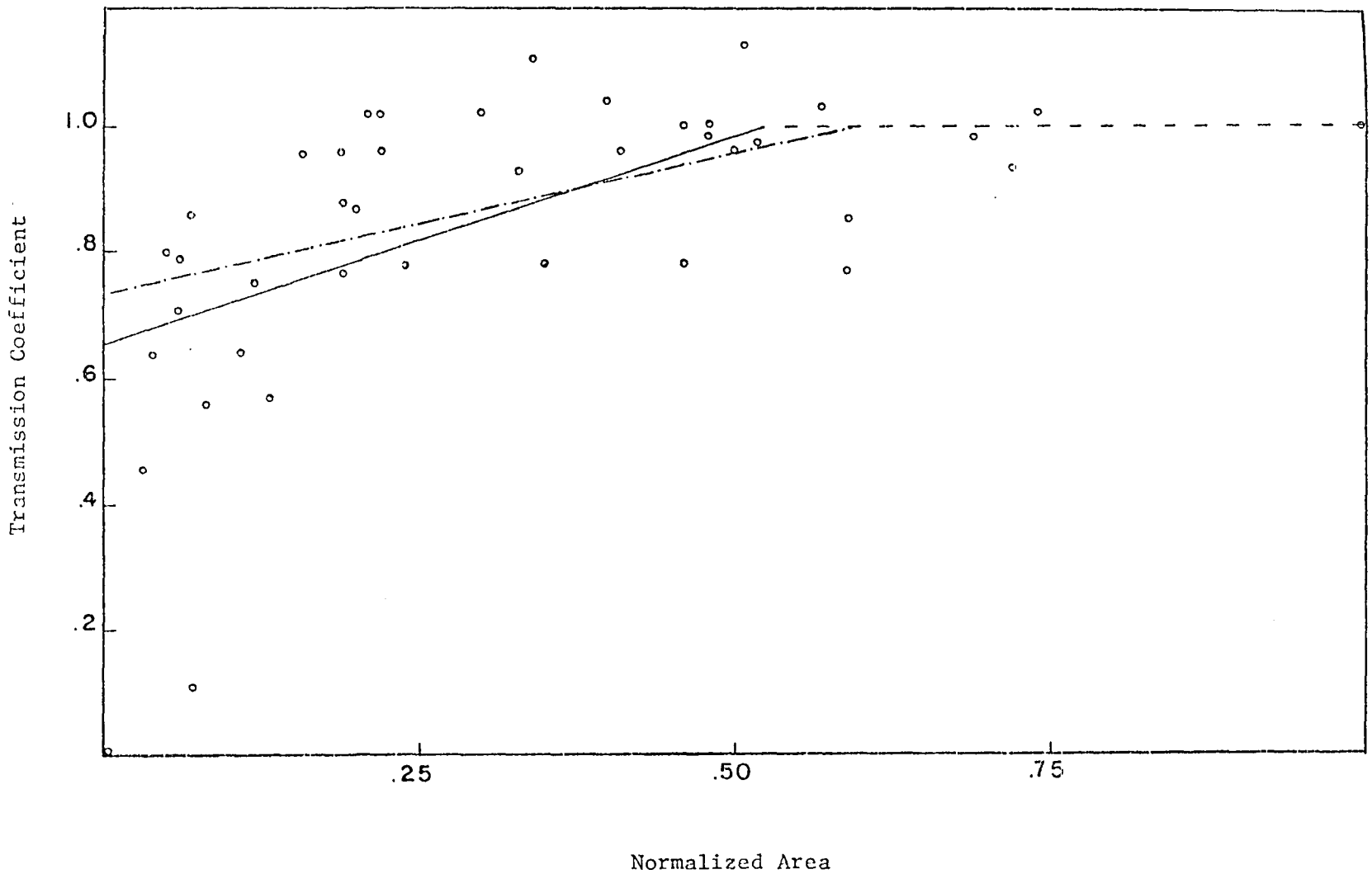

Figure 2.11 Experimental Transmission Coefficient (as determined by pin Detector) vs. Normalized Area.

degree by embalming, however there is a wide statistical variation within the samples. Drying decreases this value by approximately 20 percent, as can be seen in Table 2.4. This points to the conclusion that the water content of bone adds significantly to its viscoelastic properties. This is in agreement with the previous work reported by Laird and Kingsbury (1973) who found that bone specimens become more rigid as they lost their moisture content and the dynamic loss moduli increased approximately thirty percent over the wet condition. Bonfield and Li (1967) claimed that the initial inelastic flow occured in the collagen of bone. Since the bone mineral, hydroxyapatite, is a crystalline substance and not affected by room drying, it is reasonable to assume that the collagen of bone is the substance that is primarily affected by changes in moisture content. Therefore, the change in properties due to drying are attributable to the changes in collagen. Hence, it is not surprising to find that this damping coefficient is affected by moisture content.

It has been reported by numerous authors (Ko 1953, and Yokoo 1952) that the Young's modulus is increased when bone is dried. From the elementary theory the velocity should equal $\sqrt{E/\rho}$. Therefore, the velocity should increase as the bone is dried. However, the data in Table 2.2 and 2.4 shows that no statistically significant variation of wave velocity with moisture or embalming was observed. The reported changes by the above authors claim an increase in the elastic modulus of only twenty to thirty percent. This should give rise to an increase in velocity of nine to fourteen percent. It is conceivable that such a change was masked by the experimental error in the velocities measured here. However, it should

be noted that there is probably changes in the mass density that are not accounted for. There is also the possibility that complexities of wave propagation in wet bone cannot be adequately explained by the elementary theory.

Finally, it should be noted that the pulse width at half maximum underwent no significant broadening either in the fresh, wet or dry conditions, i.e. there was minimal dispersion of the pulse. It should be pointed out that the wave forms produced by the impact of the steel balls can be approximated by a sine squared curve, as can be seen from Figure 2.6. Now, noting that

$$\sin^2 x = \tfrac{1}{2}(1 - \cos 2x)$$

it can be seen that this pulse has only one Fourier component. Recalling that the reason that a traveling pulse becomes dispersed is because its different Fourier components all travel at different velocities. Therefore, since the pulses used here have only one component there should be no dispersion of the wave form.

Table 2.6 points out several interesting cross correlations of the data. The significant relationships obtained for a least squares fit of the data is given in Table 2.7. Of particular interest is the linear correlation between the damping coefficient (α) and the cross sectional area of the specimen (A_o).

$$A_o = .746 + 94.3\ \alpha$$

Table 2.6

Matrix of Correlations Coefficients of Experimental Parameters

N = 12, r^2/S

	F	A_o	δ	v	α	γ
Porosity (F)						
linear	-	.01	.10	.12	.1804	.0777
S =	-	NS	NS	NS	NS	NS
parabolic	-	.02	.10	.41	.3377	.2403
S =	-	NS	NS	.05	.05	NS
Area (A_o)						
linear	.01	-	.0811	.0615	.5192	.1152
S =	NS	-	NS	NS	.01	NS
parabolic	.02	-	.1890	.1763	.5869	.1585
S =	NS	-	NS	NS	.005	NS
X-ray Den. (δ)						
linear	.10	.0811	-	.0312	.0492	.1909
S =	NS	NS	-	NS	NS	NS
parabolic	.43	.2267	-	.2393	.2243	.4477
S =	.05	NS	-	NS	NS	.02
Velocity (v)						
linear	.12	.0615	.0312	-	.2627	.6466
S =	NS	NS	NS	-	NS	.002
parabolic	.13	.1250	.0350	-	.2864	.7815
S =	NS	NS	NS	-	NS	.001
Damp. Coef. (α)						
linear	.1804	.5192	.0492	.2627	-	.2128
S =	NS	.01	NS	NS	-	NS
parabolic	.2899	.5915	.0566	.5461	-	.4565
S =	NS	.005	NS	.01	-	.02
Disper Coef. (γ)						
linear	.0777		.1909	.6466	.2128	-
S =	NS		NS	.002	NS	-
parabolic	.1042		.1909	.8016	.2215	-
S =	NS		NS	.001	NS	-

NS = not significant

Table 2.7

Significant Cross Correlation Relationships

$y = A + Bx + Cx^2$, N = 12

x	y	4834	-244	7.55	.41	.05
F	v	.102	-.0101	.00028	.3377	.05
F	α	-.0084	.0106		.5192	.01
A_o	α	-.0401	.0263	-.0015	.5869	.005
		186.49	-27969	10817	.43	.05
δ	F	3.77	-4.28	1.62	.4477	.02
δ	γ	1.44	-.0012		.6466	.002
v	γ	2.17	-.0005	.00000	.7815	.001
		.746	94.3		.5192	.01
α	A_o	1.57	135	-908	.5915	.005
		2481	59573	-521144	.5461	.01
α	v	1.15	-8.43	74.1	.4565	.02
α	γ	12000	-8350		.6566	.002
γ	v	25199	-35756	13972	.8016	.001

This implies that the damping of the stress wave is related to the cross sectional area of the bone. This suggests a possible means of measuring the thinning of the bone cortex by determining the damping coefficient of the wave through a length of bone. However, the relatively small number of samples and large statistical variation of α between bone specimens would indicate the need for further tests with a much larger number of specimens.

Also of possible clinical interest is the correlation between the porosity (F) and the damping coefficient (α).

$$\alpha + .102 - .010\,F + .00028\,F^2$$

which implies that from a knowledge of the damping of a stress wave one could estimate the porosity of a bone. However, this too is subject to the warning voiced in the previous paragraph.

Simulated Fracture Healing

The results for the fracture experiments are shown in the figures above. It can be seen from them that the dispersion due to partial fracture and the transit time delay due to partial fracture rise rapidly as the point of complete fracture is approached. As this point of complete transsection is reached, there is also a rapid fall off in the transmission coefficient through the fracture site. However, it remains relatively flat up to this point. To understand this behavior consider the propagation of a stress wave across a short discontinuity as shown in

Figure 2.12. Kenner and Goldsmith (1968) give the transmission and reflection coefficients for this case as

$$T_{12} = (2\ A_1\rho_2c_2/(A_1\rho_1c_1 + A_2\rho_2c_2)) \text{ , etc.}$$

$$R_{121} = ((A_2\rho_2c_2 - A_1\rho_1c_1)/(A_1\rho_1c_1 + A_2\rho_2c_2)) \text{ , etc.}$$

Now, if region two is thin then the transit time for a wave to traverse the region may be neglected. The wavelength of our pulses is approximately ten centimeters, which is significantly larger than the width of the simulated fractures which were approximately two mm wide. Therefore, the assumption that the transit time for the pulse to cross the fracture is small is valid in our case. With this assumption, the above coefficients may be applied repeatedly to give an overall transmission coefficient through the discontinuity of

$$T_{13} = T_{12}\ T_{23}\ (1/(1 - R_{232}\ R_{212})) \qquad [2.1]$$

Now for the case being considered here region two is just the region of the bone under the cut in the cortex. Also all three regions are made of the same material, hence all the mass densities and velocities are equal. Further, since the cut was narrow the cross sectional area of regions one and three are equal. With these values for wave velocity, mass density and area the coefficients given by the authors mentioned above simplify to:

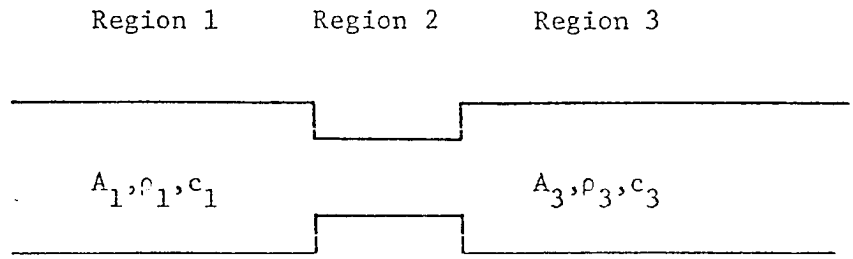

A_1, A_2, A_3 are the cross sectional areas of regions 1, 2 and 3.

ρ_1, ρ_2, ρ_3 are the mass densities of regions 1, 2 and 3.

c_1, c_2, c_3 are the wave velocities in regions 1, 2 and 3.

Figure 2.12 Wave propagation through a short discontinuity

$$
\begin{aligned}
T_{12} &= 2\,A_o/(A_o + A) \\
T_{23} &= 2\,A/(A_o + A) \\
R_{232} &= (A_o - A)/(A_o + A) \\
R_{212} &= R_{232}
\end{aligned}
\qquad [2.2]
$$

Using equations 2.2 in equation 2.1 the following transmission value is arrived at:

$$T_{13} = [4\,A_o\,A/(A_o + A)^2]\,[(A_o + A)^2/(4\,A_o\,A)] = 1$$

Thus the results of this work are in agreement with this approximate theory in the region of small fractures. For larger fractures approaching the breaking point the simplified theory breaks down and is incapable of describing the observed results. This could be due to the approximations made in the theory or due to the anisotropy or inhomogenities in the bone itself. The experimental curve of the data fitted to an exponential function for the transmission coefficients is compared to the theoretical one in Figure 2.13.

The high degree of significance of these curves (all $P << .001$) suggests the possibility of using these parameters to monitor the healing of a fractured bone. However, these measurements were only determined by the geometry of the simulated fracture. The logical extension is to determine the effects of the healing tissue or callus interposed between the geometric fracture.

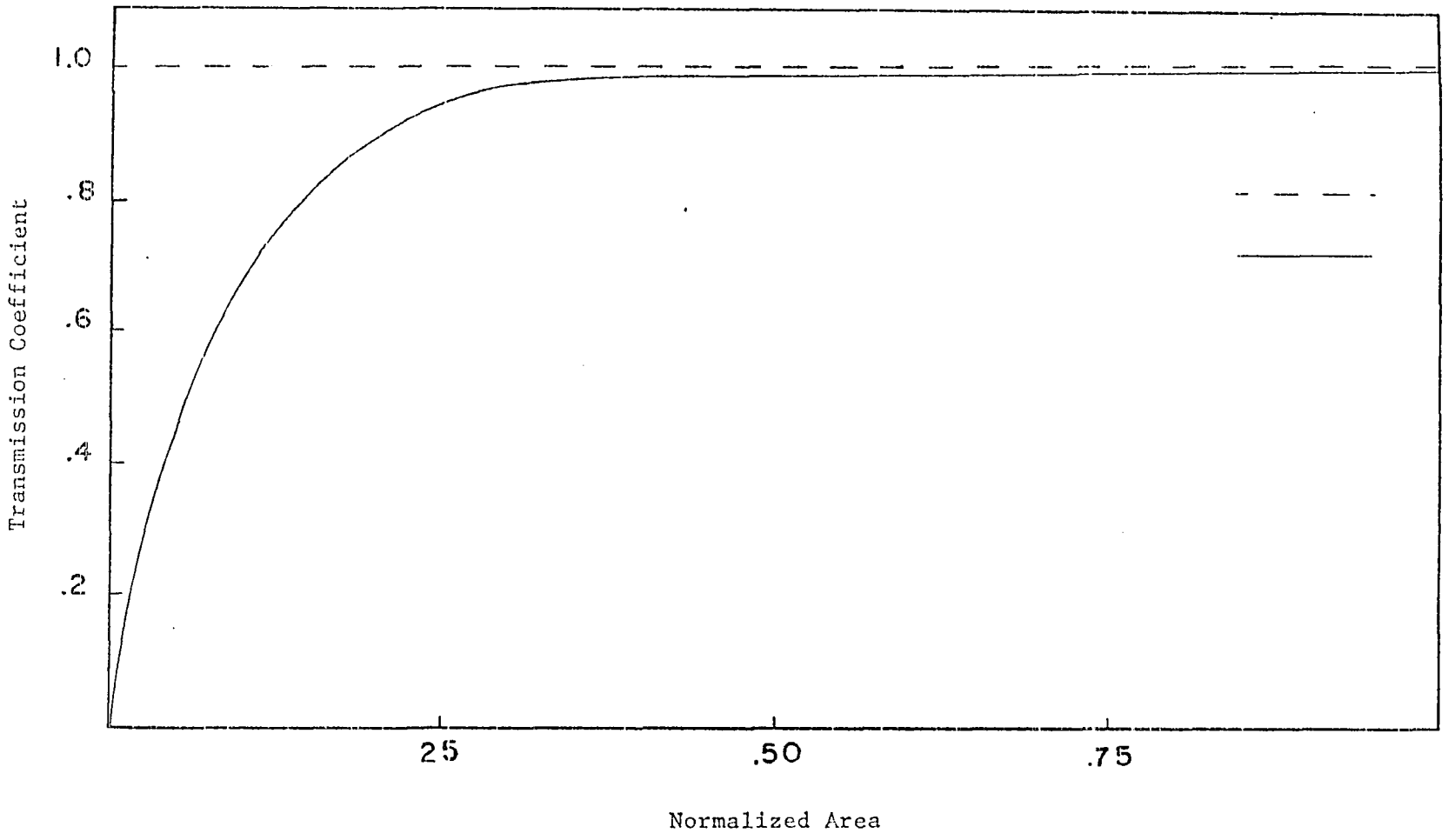

Figure 2.13 Experimental and Theoretical Transmission Coefficients vs. Normalized Area.

Skeletal Traction Pin Detector

The results from the fracture experiments were also measured with the skeletal traction pin detector. From the plot of these results in Figure 2.11 it can be seen that the fitted curve exhibits the same rapid fall off at the normalized area approaches zero that was described above for the strain gage measurements. Indeed, by comparing this plot with Figure 2.8 it can be seen that the dependence on the cross sectional area is almost identical for the two techniques used here. It has also been demonstrated that the pin detector technique is a feasible method for measuring the stress wave characteristics for a traveling wave in bone and gives results similar to those obtained from conventional strain gage techniques.

Chapter III

MATHEMATICAL MODEL OF BONE

INTRODUCTION

A knowledge of wave propagation characteristics in bone is important for our understanding of the dynamic response of the skeletal system due to an impact load. In light of this, the burgeoning amount of experimental data and the paucity of good theoretical explanations of the results, it would be advantageous to have a mathematical model of bone that encompassed the actual histology and geometry of bone.

Osseous tissue is not a uniform solid substance, but contains numerous cavities filled with bone marrow and various fluids (blood, synovial fluid, etc.). Therefore, it is not surprising that the early mathematical models of bone from a strength of materials approach have proved unsatisfactory. As pointed out in Chapter I, Nowinski and Davis have suggested that bone be treated as a poroelastic substance rather than a purely elastic one. The histology of osseous tissue indicates that this

view is a reasonable one. However, they modeled bone as a solid cylinder which made the analysis simpler but is not a realistic model of long bone.

In this study bone is modeled as a hollow circular cylinder composed of a poroelastic material and permeated with a perfect fluid. Biot's theory of poroelasticity is used to describe the material and Nowinski and Davis' (1971) approach is modified and extended. The resultant coupled differential equations are uncoupled and solved using Frobenius' method. Numerical results are obtained empirically and are compared with experimental findings.

All notation is explained in Table 3.1. Einstein's contraction notation is used throughout.

BACKGROUND - WAVES IN A POROUS MEDIUM

In his two papers on wave propagation, Biot (1956a,b) extended his theory of poroelasticity to the dynamic situation. Making the assumption that:

1. the concentration of pores per unit volume (porosity) is uniform
2. the solid is linearly and perfectly elastic; i.e. obeying Hooke's law
3. the solid undergoes small deformations
4. the liquid phase is considered a perfect fluid, i.e. its viscoelasticity is neglected

Table 3.1

Notation

$X_i^1(x,t) = X_i^1$ = displacement vector in the solid = $\hat{r}\, X_1^1 + \hat{\sigma}\, X_2^1 + \hat{\delta}\, X_3^1$

$X_i^2(x,t) = X_i^2$ = displacement vector in the fluid = $\hat{r}\, X_1^2 + \hat{\sigma}\, X_2^2 + \hat{\delta}\, X_2^2$

$\hat{r}$, $\hat{s}$, $\hat{\delta}$ are unit vectors

ε^1 = strain in solid

ε^2 = strain in fluid

ρ_s = mass density of solid

ρ_f = mass density of fluid

ρ_ℓ = mass density of fluid per unit volume of aggregate

$\rho_{11} = \rho_s + \rho_\ell$

$\rho_{12} = \rho_f + \rho_\ell$ = mass coupling parameter

$\rho_{22} = -\rho_\ell$

f = porosity

K = inverse of bulk modulus under constant pore pressure

ζ = coefficient of unjacketed compressability

ξ = coefficient of fluid content

λ = Lamé constant $= A - \frac{Q^2}{R}$

μ = Lamé constant

$Q = (1 - \quad - \zeta/K)/(\xi + \rho - \zeta^2/K)$

$R = {}^2/(\xi + \rho - \rho^2/K)$

$P = A + 2\mu$

$s = Q\,\varepsilon^1 + R\,\varepsilon_2^2$

$\rho_1^* = \rho_{11}\, P^2 - \rho_{12}\, P^2/\rho_{22} - \mu\gamma^2$

$\rho_2^* = \rho_{11}\, P^2 - \rho_{12}^2\, P^2/\rho_{22}$

$E^* = [(P - \rho_{12}/\rho_{22}\, Q)\psi^1 + (Q - \rho_{12}/\rho_{22}\, R)\psi^1]$

5. the pores are interconnected;

6. the stress in the bulk is uniformly divided between the solid and liquid phase.

Biot obtained the following wave equations for a poroelastic material

$$\mu X^1_{j,ii} + [(A + \mu)\, \varepsilon^1 + Q\varepsilon^2]_{,j} = \frac{\partial^2}{\partial + 2} (\rho_{11} X^1_j + \rho_{12} X^2_j)$$

$$j = 1,2 \quad [3.1]$$

$$[Q\, \varepsilon^1 + R\, \varepsilon^2]_{,j} = \frac{\partial^2}{\partial + 2} (\rho_{12} X^1_j + \rho_{22} X^2_j)$$

where

$$\varepsilon^j = X^j_{i,i} \qquad j = 1,2 \quad [3.2]$$

By applying the divergence operator, dilational waves can be separated out to give

$$[P\, \varepsilon^1 + Q\, \varepsilon^2]_{,ii} = \frac{\partial^2}{\partial + 2} (\rho_{11}\, \varepsilon^1 + \rho_{12}\, \varepsilon^2)$$

$$j = 1,2 \quad [3.3]$$

$$[Q \quad + R \quad]_{,ii} = \frac{\partial^2}{\partial + 2} (\rho_{12}\, \varepsilon^1 + \rho_{22}\, \varepsilon^2)$$

Similarly the curl operator can be applied to give the rotational waves if desired.

POROELASTIC WAVES IN BONE

Formulation

We will consider bone to be a hollow circular cylinder composed of a poroelastic material with inner radius = b and outer radius = a. Assuming a sinusoidal wave of frequency = p and wave number = γ propagating down the cylindrical axis we have:

$$X_n^j(x,t) = \Xi_n^j(r) \exp[i(\gamma\delta + pt)]$$

where $n,j = 1,2$ [3.4]

$\Xi_n^j(r)$ = radial dependence of solution

Using this and equation 3.2 in equation 3.3 we find that

$$\varepsilon^1_{,11} + \frac{1}{r}\varepsilon^1_{,1} + (\beta_1 p^2 - \gamma^2)\varepsilon^1 + \beta_2 p^2 \varepsilon^2 = 0$$

$$\varepsilon^2_{,11} + \frac{1}{r}\varepsilon^2_{,1} + (\beta_3 p^2 - \gamma^2)\varepsilon^2 + \beta_4 p^2 \varepsilon^2 = 0$$

where

$$\beta_1 = \frac{Q\rho_{12} - R\rho_{11}}{\alpha} \qquad \beta_2 = \frac{Q\rho_{22} - R\rho_{12}}{\alpha}$$

$$\beta_3 = \frac{(A + 2)\rho_{22} - Q\rho_{12}}{\alpha} \qquad \beta_4 = \frac{(A + 2\mu)\rho_{12} - Q\rho_{11}}{\alpha}$$

$$\alpha = Q^2 - R(A + 2\mu)$$

Now matters can be simplified by letting

$$\psi^j = X^j_{1,1} + \frac{1}{r} X^j_1 + k\,\gamma\, X^j_3 \qquad j = 1,2 \qquad [3.5]$$

We then get the coupled differential equations

$$\psi^1_{,11} + \frac{1}{r}\psi^1_{,1} + \gamma_1\psi^1 + \beta_2 p^2\psi^2 = 0$$

$$\psi^2_{,11} + \frac{1}{r}\psi^2_{,1} + \gamma_2\psi^2 + \beta_4 p^2\psi^1 = 0$$

where

$$\gamma_1 = \beta_1 p^2 - \gamma^2$$

$$\gamma_2 = \beta_3 p^2 - \gamma^2 \qquad [3.6]$$

Equations 3.5 and 3.6 can then be combined to uncouple the two differential equations to give:

$$r^3\psi^1_{,1111} + 2r^2\psi^1_{,111} + [(\gamma_1+\gamma_2)r^3 - r]\psi^1_{,11}$$

$$+ [(\gamma_1+\gamma_2)r^2 + 1]\psi^1_{,1} + (\gamma_1\gamma_2 - \beta_2\beta_4 p^4)r\,\psi^1 = 0$$

Solution

Nowinski and Davis have shown that this fourth order differential equation possesses a fundamental set of solutions which are regularly behaved at the origin. We will therefore proceed to solve this equation using Frobenius' method of power series. Assuming a power series expansion of the form

$$\psi^1(r) = C_n r^{n+\delta}$$

We obtain an indicial formula from which the general solution is found to be

$$(r) = A_n r^n + B_n r^n \ln r/a$$

where the recurrence relationship gives us

$$A_n = c_n + \frac{\partial c_n}{\partial \delta} \qquad n > 2$$

$$B_n = -c_n \ln a \qquad N > 2$$

†

$$= -c_{n-2} (\gamma_1 + \gamma_2) (\delta + n-2)^2 - c_{n-4} (\gamma_1\gamma_2 - \beta_2\beta_4 p^4)^4 \Big| \delta = 0$$

$$c_n = 0$$

Where A_o, A_2, B_o, B_2 are determined by the boundary conditions.

The boundary conditions, i.e. that the surfaces are free from external traction and permeable to the fluid are

$$\sigma_{11} = \sigma_{13} = s = 0 \qquad r = a,b$$

which can be expressed as

$$2\mu X^1_{1,1} + A \psi^1 + Q\psi^2 = 0$$

$$i \gamma X^1_1 + X^1_{3,} = 0 \qquad r = a,b$$

$$Q \psi^1 + R \psi^2 = 0$$

---

†This differs from Nowinski and Davis result and they have concurred that these are the correct formulae (Davis - private communication).

We can combine two of these equations to eliminate the displacement terms to give as two remaining boundary conditions dependent only on ψ^1 and ψ^2

$$+ (2\mu^2\gamma^2/(\rho_1^* - \mu\gamma^2) + 2\mu)\, E_{,11} + A\rho_1^*\, \psi^1 + Q\rho_1\, \psi^2 = 0$$

$$r = a,b$$

$$Q\, \psi^1 + R\, \psi^2 = 0$$

We have four equations and four unknowns (A_o, A_2, B_o and B_2) and the problem is thus theoretically soluble. Now making the approximation that only terms of order r^2 need be considered for a first estimate we obtain

$$\psi^1 \approx A_o + A_2 r^2 + B_o \ln r/a + B_2 r^2 \ln r/a$$

In order for a nontrivial solution to a set of homogenous equations to exist the determinant of the coefficient matrix must vanish.

$$e_{ijk} A_{1j} A_{2j} A_{3k} = 0 \qquad [3.7]$$

(See Table 3.2 for the values of A_{ij}.)

The resultant expression thus gives us a relationship between the variables of the theory and the wave velocity.

RESULTS

Elastic Limit

To test the validity of the above expression the limiting case of a solid cylinder as the material approaches a perfectly elastic condition

Table 3.2

Elements of Coefficient Matrix

$A_{11} = A\,\rho_1^* - F_2\gamma_2$ $\qquad A_{12} = F_1(2q_1 - F_3 2\gamma_1) + A\,\rho_1^* a^2 - F_2(4 + \gamma_1 a^2)$

$A_{13} = F_1(-q_1/a + F_3\gamma_1/a^2)$ $\qquad A_{14} = F_1(3q_1 - F_3[-4/a + 3\gamma_1 a]) - 4F_2$

$A_{21} = A\,\rho_1^* - F_2\gamma_1$ $\qquad A_{22} = F_1(2q_1 - 2\gamma_1 F_3) + A\,\rho_1^* b^2 - F_2(4 + \gamma_1 b^2)$

$A_{23} = F_1(-q_1/b^2 + F_3\gamma_1/b^2) + A\,\rho_1^* \ln b/a - F_2\gamma_1 \ln b/a$

$A_{24} = F_1(2q_1 \ln b/a + 3q_1 - F_3[-4b^2 + 2\gamma_1 \ln b/a + 3\gamma_1 b])$

$\qquad + A\,\rho_1^* b^2 \ln b/a - F_2(4 \ln b/a + 4 + \gamma_1 b^2 \ln b/a)$

$A_{31} = Q - R\gamma_1/\beta_2 p^2$ $\qquad A_{32} = Qa^2 - R/\beta_2 p^2\,(4 + \gamma_1 a^2)$

$A_{33} = 0$ $\qquad A_{34} = -4\,R/\beta_2 p^2$

$A_{41} = A_{31}$ $\qquad A_{42} = Qb^2 - R/\beta_2 p^2\,(4 + \gamma_1 b^2)$

$A_{43} = Q \ln b/a - R/\beta_2 p^2\,\gamma_1 \ln b/a$

$A_{44} = Q\,b^2 \ln b/a - R/\beta_2 p^2\,(r \ln b/a + 4 + \gamma_1 b^2 \ln b/a)$

where

$F_1 = 2\mu^2\gamma^2/(\rho_1^* - \mu\gamma^2) + 2\mu$ $\qquad F_2 = Q\,\rho_1^*/(\beta_2 p^2)$

$F_3 = q_2/(\beta_2 p^2)$

is considered. In this situation

$$\rho_{12} = \rho_{22} = 0 \qquad \rho_{11} = \rho = \text{mass density}$$

$$Q = \beta_2 = 0 \qquad \beta_1 = \rho \,/\, (A + 2\mu)$$

With this in mind the dispersion relationship becomes

$$p^4(-4\mu\ \rho\ q_2\beta_1) + p^2(4\mu\ \rho\ q_2\gamma^2 + 4\mu^2\gamma^2\ q_2\beta_1) - 4\mu^2\gamma^4\ q_2 = 0$$

which simplifies to (where $v = p/\gamma$ = velocity)

$$v^4 - v^2\ (\gamma + 3\mu)/\rho + \mu(\gamma + 2\mu)\rho^2 = 0$$

this gives us

$$v_1 = \pm\sqrt{\mu/\rho}$$

$$v_2 = \pm\sqrt{(\gamma + 2\mu)/\rho}$$

That is we have two waves traveling along the z axis in the positive direction with wave velocities v_1 and v_2 and two waves traveling along the z axis in the negative direction with wave velocities v_1 and v_2. It should be noted that v_1 and v_2 are exactly the expressions obtained for the dilational and distortional wave velocities.

Dissipative Forces

If dissipative forces are introduced into the consideration Biot's wave equations become

$$\mu X_{j,kk} + [(A + \mu)\varepsilon^1 + Q\,\varepsilon^2]_{,j} = \frac{\partial^2}{\partial +^2} (\rho_{11} X_j^1 + \rho_{12} X_j^2)$$

$$+ b \frac{\partial}{2+} (X_j^1 - X_j^2) \qquad j = 1,2$$

$$[Q\,\varepsilon^1 + R\,\varepsilon^2]_{,j} = \frac{\partial}{\partial +^2} (\rho_{12} X_j^1 + \rho_{22} X_j^2) - b \frac{\partial}{\partial +} (X_j^1 - X_j^2)$$

where

b = $\nu f^2/k$

k = Darcey's coefficient of permeability

ν = fluid viscosity

f = porosity

Now assuming a sinusoidal wave as in equation 3.4 above we obtain the new relationships

$$\mu X_{j,ii}^2 + [(A + \mu)\varepsilon^1 + Q\,\varepsilon^2]_{,j} = \frac{\partial}{\partial +^2} (\rho_{11} X_j^1 + \rho_{12}^1 X_j^2)$$

$$[Q\,\varepsilon^1 + R\,\varepsilon^2]_{,j} = \frac{\partial}{\partial +^2} (\rho_{12} X_j^1 + \rho_{22} X_j^2) \qquad j = 1,2$$

where

$$\rho_{11}^1 = \rho_{11} - bi/p$$

$$\rho_{12}^1 = \rho_{12} + bi/p$$

$$\rho_{22}^1 = \rho_{22} - bi/p$$

It should be noticed that this is the same expression as equation 3.1 with ρ_{ij}^1 substituted for ρ_{ij}.

Numerical Results

Equation 3.7 yields an intricate formula for the wave number which is dependent on several variables such as the wave frequency, the inner and outer radii of the cylinder and the porosity as well as the physical constants of the material the cylinder is composed of. This formula was manipulated to make it suitable for programming into an IBM 370 computer. The numerical results reported below were obtained from this program and are plotted as a function of several dimensional variables.

For simplicity of presentation, we define the following quantities, a dimensionless velocity (V):

$$V = \upsilon/\upsilon_o$$

where $\upsilon_o = \sqrt{E/\rho}$

a dimensionless ratio of radii (b/a)

$$b/a = \text{inner radius/outer radius}$$

a dimensionless frequency (ν)

$$\nu = p/p_o$$

where $p_o = \upsilon_o \gamma_o$

$$\gamma_o = 1 \text{ cm}^{-1}$$

With all other variables held constant the porosity was varied over

the range from 0 to 45 percent. The resultant solutions are shown in figure 3.1 for several values of b/a. It can be seen that in general there are two solutions for each value of b/a. This is in agreement with Biot (1955a) who found that there were two dilational waves in a porous material, one of which is highly attenuated, and with Nowinski and Davis (1971) who also found two solutions.

Similarly, with all other variables held constant the wave numbers were varied to find their frequency dependence. The solutions for several values of b/a are shown in figure 3.2 as a function of the dimensionless frequency (υ). It should be noted that each set of solutions corresponding to a value of b/a has a solution in which the wave number is linearly related to the frequency. For these solutions the theory predicts no dispersion of the waves. There is also a set of solutions where the relationship is nonlinear. For these solutions a dispersion is predicted.

Figure 3.3 depicts the relationship of the theoretical wave velocities as a function of radius for several values of b/a.

Figure 3.4 shows the results of experimentally measured wave velocities versus measured porosity. By comparing this plot with figure 3.1 it can be seen that the experimental results are consistent with the velocities predicted by the theory[†]. Further, the experimental work of

---

[†]It is reasonable to assume that we are measuring the dilational wave velocity and not the distortional or Rayleigh wave velocities. This is true because the experimental velocities cluster around the value predicted for dilational waves by the Pochammer theory (υ_o) while the distortional and Raleigh wave velocities would be much less than this value (.63 υ_o and .58 υ_o respectively).

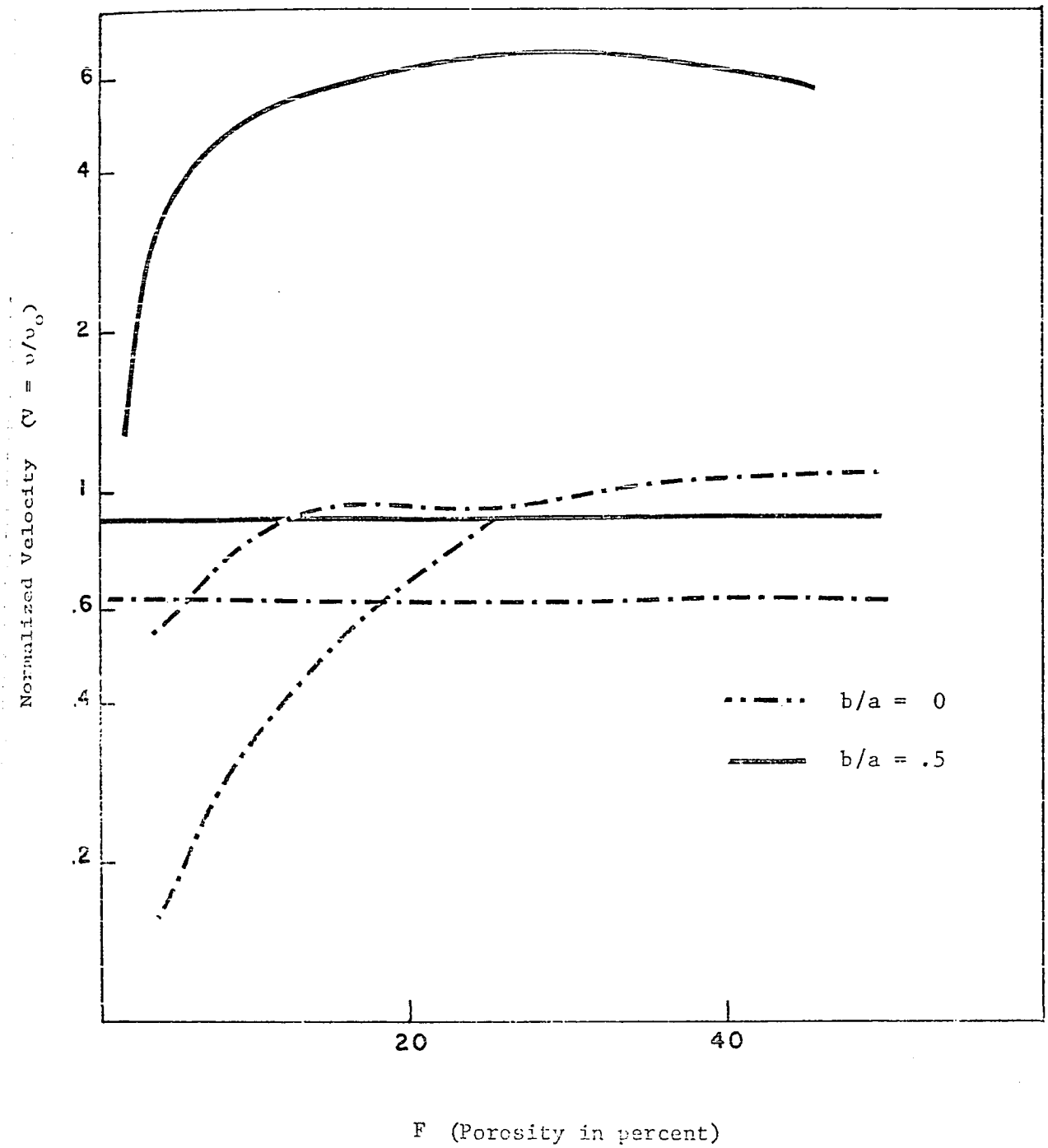

Figure 3.1 Theoretical velocity vs. porosity.

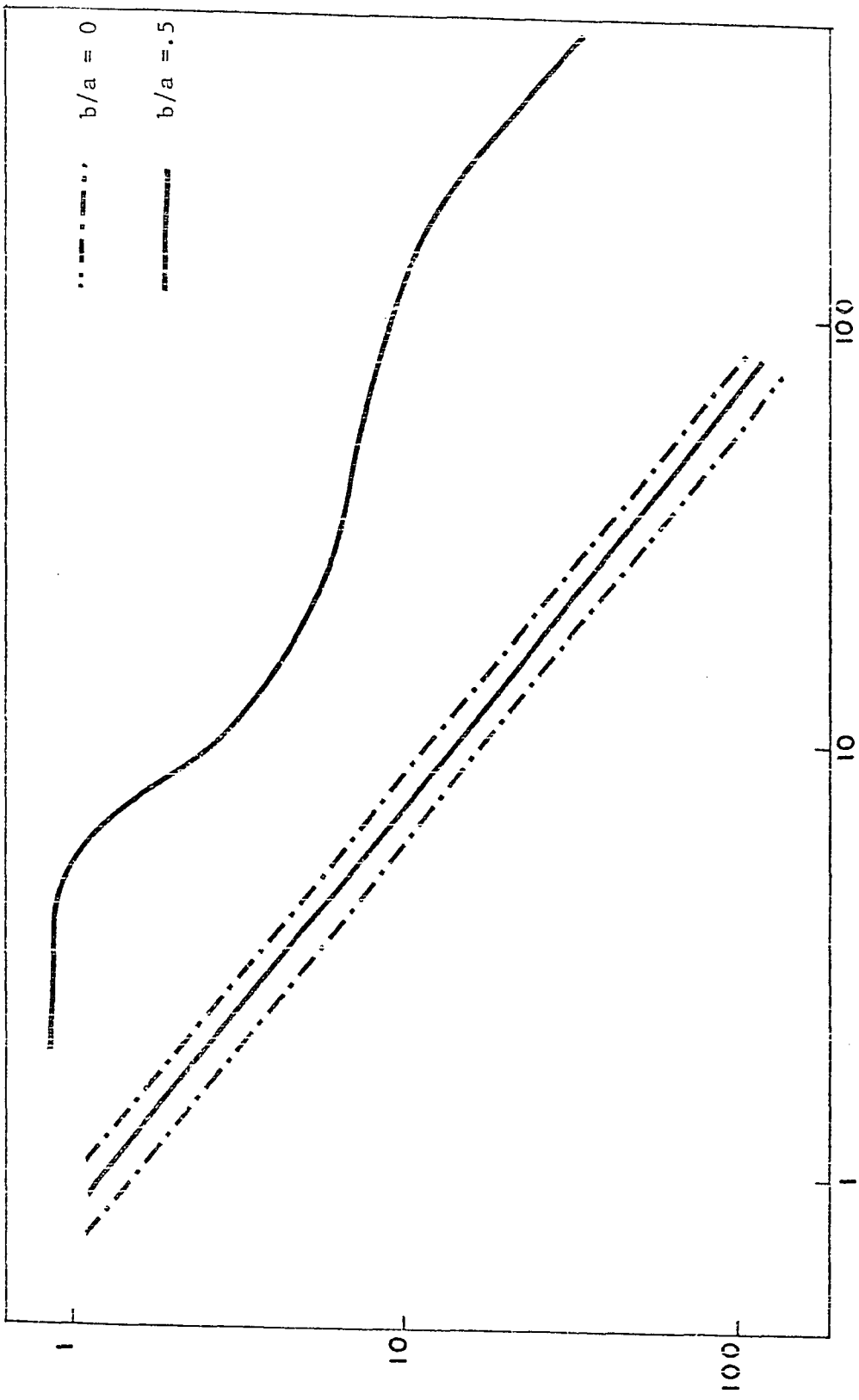

Figure 3.2 Theoretical wave number vs. Frequency.

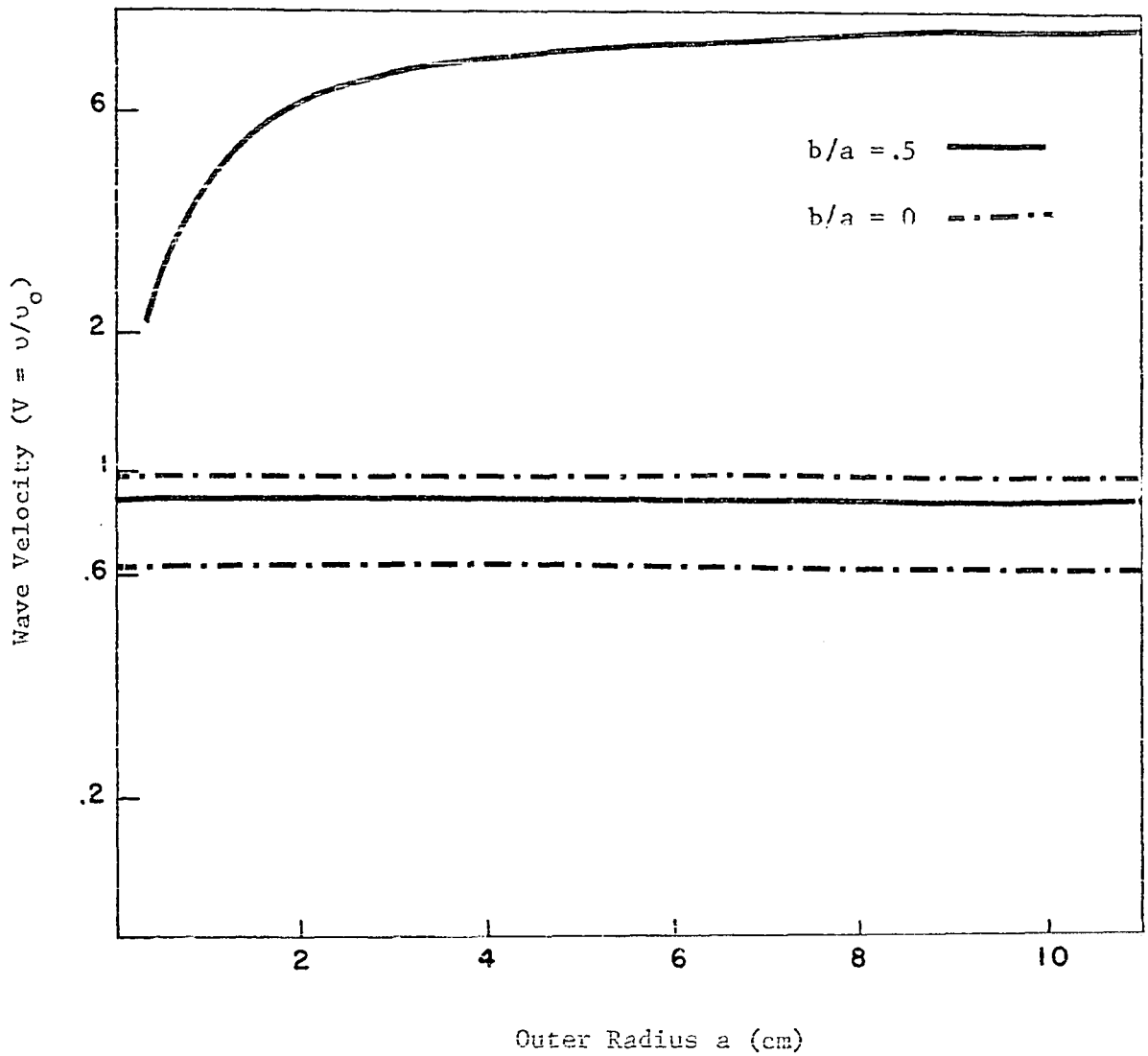

Figure 3.3 Theoretical wave velocity vs. outer radius of bone.

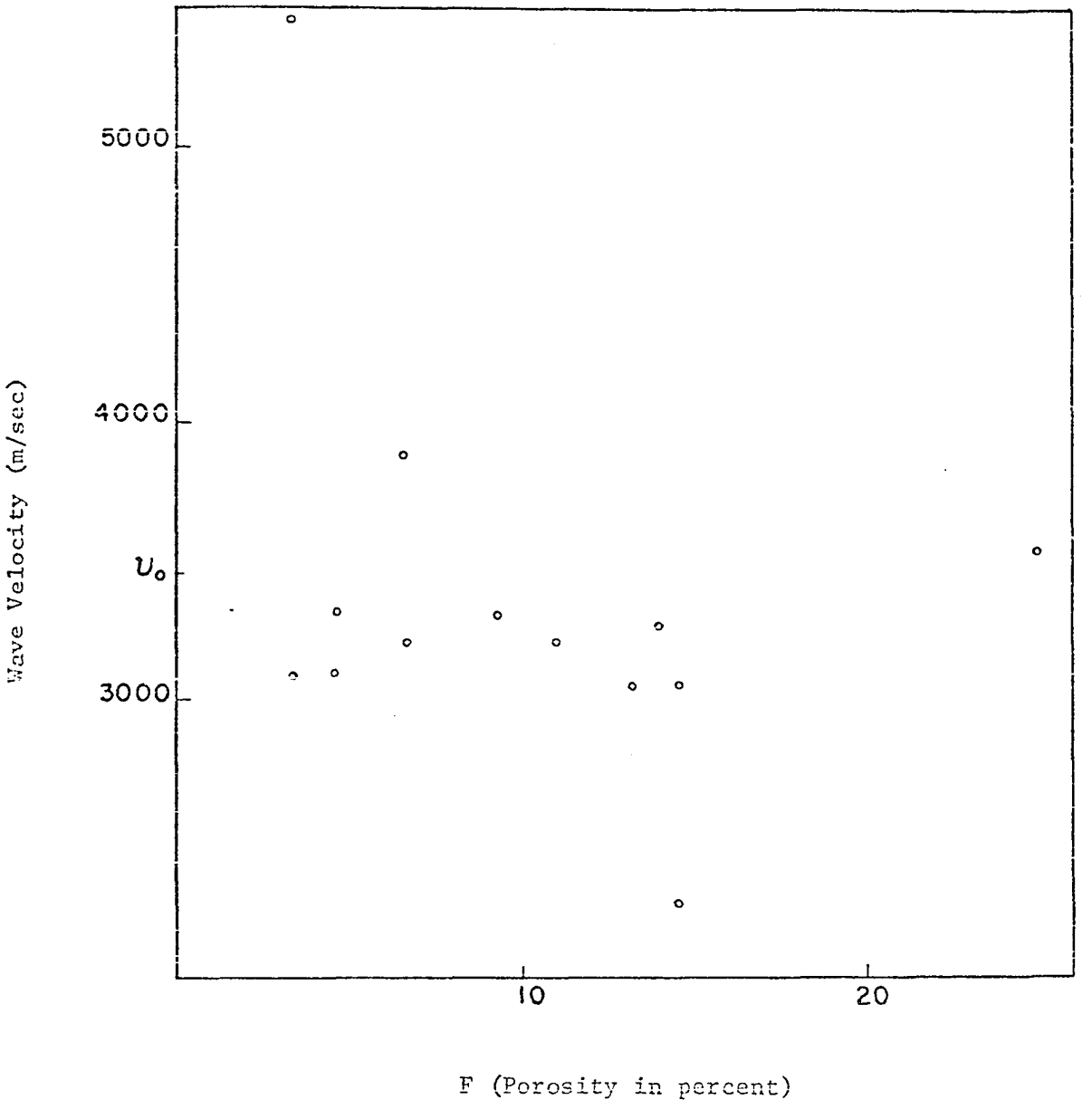

Figure 3.4 Experimental wave velocity vs. measured porosity.

others have found the wave velocities to be in this range. However, the fine variations in velocity that the theory predicts for changes in porosity cannot be thoroughly evaluated by this set of data due to its limited size, the possible effects that variations in the Young's modulus and mass density between bone specimens, and non-cylindrical geometry play in changing the expected velocity.

We have examined a model of bone which has the advantage of being able to encompass the porous nature of bone. Although other models, an empiric viscoelastic one for example, might be able to predict the dynamic behavior of bone equally well, this model takes into account the porosity directly. Thus, the effects of a clinically interesting and important property can be uniquely examined. However, in modeling bone as has been done above several assumptions have been made. Although these are reasonable approximations, they do not entirely describe the complex system that osseous tissue truely is. A partial ennumeration of the areas of discrepancy between the model and physical reality would include the fact that bone is not a hollow cylinder, but is irregularly structured with varying substances in its inner core. Also no account was taken of the composite nature of bone or its microstructure other than its porous nature. Further, not all the pores are interconnected and bone is definitely anisotropic not isotropic as assumed in the theory. It can be seen that there are many areas for further modification of the theory to more closely approximate the actual specimen. However, the present model does provide a useful tool for understanding the effects of bone porosity.

Chapter IV

CONCLUSIONS AND FUTURE RESEARCH

In summary, experiments were performed on intact human long bone using dynamic compressional waves induced by small amplitude impacts to determine the elastic wave propagation characteristics of bone. The viscoelastic damping was measured and found to be comparable for fresh and wet embalmed bone, but decreased for dry embalmed bone. This value is important since techniques that attempt to make use of the wave damping characteristics for clinical purposes, such as measuring the transmission coefficient through a fracture site to monitor healing, must take into account this natural damping that occurs in normal bone. The results would also seem to indicate that wet embalmed bone may be used in place of fresh bone for some dynamic tests. However, more specimens of wet embalmed and fresh bone need to be tested before this can be verified. Velocity and dispersion measurements were also made which should also prove to be useful for future clinical applications.

A first approximation model of bone fractures by serial cuts into

the cortex were also performed. These provided some basic information on the effects of a short discontinuity on the transmission coefficient, dispersion and transit time delay of a wave pulse. This demonstrated the feasibility of using this technique for obtaining clinical information as well as providing some basic data that would be necessary for the application of such a technique.

A new technique for measuring stress wave propagation was also investigated. This method made use of Faraday's principle that a moving wire in a magnetic field will generate a voltage difference across the wire. In place of a wire a skeletal traction pin, such as is used in some cases of bone fracture was used. The results shows the feasibility of the method in giving data comparable to that obtainable from conventional strain gage methods. Thus, it may be possible to use this technique as an in vivo method of measuring stress wave characteristics.

The problem of incorporating bone's porosity into a theory of wave propagation was approached using Biot's theory of poroelasticity. A first order approximation was solved and found to be consistent with the experimental findings of this work and the findings of others. However, the fine structure variations predicted by the theory are beyond the level of resolution of this project. It is also felt that the general theory for a hollow cylinder leads to an exceedingly cumbersome set of formulae. However, the simplified solution for a solid cylinder was workable and should be investigated further for the effects of higher order terms and for dissipative materials. This will prove to be useful if it becomes practical to use wave propagation as a diagnostic test of osteoporosis.

Work is also being done on developing techniques that would be capable of measuring stress wave characteristics in the in vivo situation. This includes the investigation of the practicality of the magnetic traction pin detector in in vivo tests by performing measurements on rabbits with fractured tibias using this method. These tests suggested several modifications that should be made for in vivo testing. Also, others are testing techniques that will provide a shorter pulse width and make use of the piezoelectric effect to measure the traveling wave pulse. Preliminary results from a series of measurements similar to those described above but using a PCB accelerometer have demonstrated results similar to those described above.

Future research in this area could prove to be extremely fertile. The most immediate need for work lies in several areas. A more accurate model for bone fracture that takes into account the difference in mechanical impedence between the fracture callus and normal bone as well as the geometric discontinuity needs to be considered. A logical next approximation is to experimentally fracture animal bones and at set time intervals sacrifice the animal. In this way specimens of fresh bone with fractures at various stages of healing can be obtained. By repeating the tests bone in this work on wave velocity, transmission coefficient, dispersion and transit delay the effects of the difference in the mechanical impedence of the callus could be measured as desired. Once this is completed, the experimentation could be extended to in vivo testing in animal and human tests. This could be done using one of the techniques described above.

Thus, some of the ground work has been laid for the establishment of a new diagnostic technique using the stress wave propagation properties of bones. It is felt that with the data accumulated here and in future research a feasible method could be derived that would prove useful to the researcher and clinician. However, further work especially in vivo animal experimentation is necessary to gain confidence in this technique before this method can be used clinically to evaluate fracture healing.

APPENDIX

Common Symbols

σ	stress
ε	strain
t	time
E	Young's modulus
ρ	mass density
r^2	coefficient of determination
S	significance level
F	porosity
c,v	wave velocity
B	magnetic field
α	damping coefficient
A/A_o	normalized area of partially fractured bone specimen
T	transmission coefficient
D	broadening ratio of wave pulse
Δ	transit time delay of wave pulse
T_{pin}	transmission coefficient (as measured by pin detector)
δ	radiographically determined mineral density
γ	relative pulse width or broadening in intact bone

Fracture Data

	A/A_o	T	T_{pin}	Y	Δ
(12)	1.00	1.00	1.00	1.00	0.0
	.76	.97		1.11	2.0
	.74	.99	1.01	1.00	.8
	.72	1.14	.93	.88	.8
	.69	1.04	.98	.81	1.2
	.59	.99	.85	1.16	7.2
	.59	1.01	.77		
	.57	.73	1.03	.94	1.6
	.53	1.05		1.04	1.2
	.52	.78	.97	1.02	
	.51	1.06	1.13	1.05	4.8
	.50	.99	.96	1.07	3.2
	.48	.66	1.00	1.16	8.0
	.48	.84	.99	1.04	4.4
	.46	.83	.78	.90	5.2
	.46	.77	1.00	1.02	
	.41	1.01	.96	1.09	4.8
	.40	.90	1.04	1.24	.8
	.35	.87	.78	.94	9.6
	.34	1.03	1.11	1.13	18.4
	.33	.72	.93	1.09	15.6
	.31	.75		1.10	1.4
	.30	1.06	1.02	1.07	15.7
	.24	.95	.78	.93	16.0
	.22	.76	.96	1.30	28.4
	.22	.47	.77	1.13	15.6
	.22	.39	1.02	1.06	14.8
	.21	1.01	.75	1.24	34.8
	.20	.96	.87	1.15	14.0
	.19	.52	.96	1.05	23.6
	.19	.66	.88	1.03	18.8
	.16	.92	.96	1.12	19.2
	.13	.98	.57	1.22	26.0
	.12	.69	.64	1.47	
	.11	.58	.64	1.33	29.2
	.10	.55		1.38	8.0
	.08	.33	.56	1.05	48.0
	.07	.57	.86	1.24	33.2
	.07	.04	.11		
	.06	.45	.79	1.13	29.6
	.06	.48	.71	1.01	42.0
	.05	.49	.80	1.27	29.1
	.05	.15			82.0
	.04	.32			56.0
	.03	.46	.46	1.60	36.0
(12)	.00	.00	.00		

BIBLIOGRAPHY

Abendschein, W. and Hyatt, G. (1970). Ultrasonics and selected physical properties of bone. Clinical Orthopaedics 69, 294-301.

Abramovich, A. (1970). Effects of ultrasound on the tibia of the young rat. J. Dent. Res. 49, 5, 1182.

Anast, G., et al. (1958). Ultrasonic technique for the evaluation of bone fractures. Amer. J. Phys. Med. 37, 157-159.

Armenakas, A. (1967). Propagation of harmonic waves in composite circular cylindrical shells. I: theoretical investigations. AIAA. J. 5, 740-744.

Ascenzi, A. and Bell, G. (1972). Bone as a mechanical engineering problem. The Biochemistry and Physiology of Bone. Vol. 1, 2nd ed. Academic Press, N.Y. 311-352.

Ascenzi, A. and Bonucci, E. (1964). The ultimate strength of single osteons. Acta Anat. (Basel) 58, 160-183.

Ascenzi, A. and Bonucci, E. (1967). The tensile properties of single osteons. Anat. Rec. 158, 375.

Ascenzi, A. and Bonucci, E. (1968). The compressive properties of single osteons. Anat. Rec. 161, 377.

Ascenzi, A., et al. (1966). The tensile properties of single osteons studied using a microwave extensometer. Studies on the Anatomy and Function of Bone and Joints (Ed. by F. Evans), Springer-verlag, Heidelberg, 121-141.

Askew, M., et al. (1973). Analysis of the intraosseous stress field due to compression plating. Proceedings of the 26th ACEMB Conf.

Barnes, G. and Pinder, D. (1974). In vivo tendon tension and bone strain measurements and correlation. J. Biomech. 7, 35-42.

Barnes, G., et al. (1975). Response to the letter to the editors of Dr. S. Salmons. J. Biomech. 8, 88.

Bartholomew, R. and Torvik, P. (1972). Elastic wave propagation in filamentary composite materials. Int. J. Solids Structures 8, 1389-1405.

Bassett, C. (1965). Electrical effects in bone, Sci. Amer. 213, 4, 18.

Bassett, C. (1965). Electromechanical factors regulating bone architecture. 3rd European Symp. Cal. Tissues, 78-89.

Beneviste, Y. and Lubliner, J. (1972). Perturbation solutions for wave propagation in nonlinearly elastic rods. Int. J. Solids Structures, 8, 1115-1138.

Bevington, P. (1969). Data Reduction and Error Analysis for the Physical Sciences. McGraw-Hill, Inc., N.Y.

Bickford, W. and McGlothin, G. (1970). Stress wave propagation in inhomogeneous cylinders. J. Sound Vib. 12, 4, 467-474.

Biot, M. (1941). General theory of three-dimensional consolidation. J. Appl. Phy. 12, 155-164.

Biot, M. (1955a). Theory of propagation of elastic waves in a fluid saturated porous solid. I. Low frequency range. J. Acoust. Soc. Amer. 28, 2, 168-178.

Biot, M. (1955b). Theory of propagation of elastic waves in a fluid saturated porous solid. II. Higher frequency range. J. Acoust Soc. Amer. 28, 2, 179-191.

Biot, M. (1955c). Theory of elasticity and consolidation for a porous anisotropic solid. J. Appl. Phy. 26, 2, 182-185.

Biot, M. (1962). Mechanics of deformation and acoustic propagation in porous media. J. Appl. Phy. 33, 4, 1482-1498.

Biot, M. and Willis, D. (1957). The elastic coefficients of the theory of consolidation. J. Appl. Mech. 24, 594-601.

Bird, F., et al. (1968). Experimental determination of the mechanical properties of bone. Aerospace Med. 39, 44-48.

Black, J. and Korostoff, E. (1973). Dynamic mechanical properties of viable human cortical bone. J. Biomech. 6, 435-438.

Bloom, W. and Fawcett, D. (1968). A Textbook of Histology. 9th ed. W. B. Saunders Co., Philadelphia.

Bogy, D. and Naghdi, P. (1969). On heat conduction and wave propagation in rigid solids. Office of Naval Research Report No. AM-69-6.

Bonfield, W. and Clark, E. (1973). Elastic deformation of compact bone J. Mat. Sci. 8, 1590-1594.

Bonfield, W. and Li, C. (1966). Deformation and fracture of bone. J. Appl. Phy. 37, 2, 869-875.

Bonfield, W. and Li, C. (1967). Anisotropy of nonelastic flow in bone. J. Appl. Phy. 38, 6, 2450-2455.

Bonfield, W. and Li, C. (1968). The temperature dependence of the deformation of bone. J. Biomech. 1, 323-329.

Booker, R. and Sagar, F. (1970). Velocity dispersion of the lowest order longitudinal mode in finite rods of circular cross section. J. Acoust. Soc. Amer. 49, 5, 1491-1498.

Bourgois, R. and Burny, F. (1972). Measurement of the stiffness of fracture callus in vivo. A theoretical study. J. Biomech. 5, 85-91.

Braden, T. and Bronker, D. (1973). Effect of certain fixation devices in functional limb usage in dogs. J.A.V.M.A. 162, 8, 642-646.

Brown, S. and Mayor, M. (1974). Some ultrasound properties of healing fractures. Proceedings of the 2nd Annual N.E. Bioengng. Conf.

Brusilovskaia, G. and Ershov, L. (1974). Dynamics of a hollow symmetrically circular elastic cylinder. J. Appl. Math. Mech. PMM 38, 3, 520-523.

Burturla, E. and Pope, M. (1973). A finite element wave propagation model of pathogenic and healing bone. Proc. 1973 N.E. Biomech. Conf., 36-45.

Campbell, J. and Jurist, J. (1971). Mechanical impedance of the femur: a preliminary report. J. Biomech. 4, 319-322.

Campbell, J. and Pond, M. (1972). Repair of fractures of the distal humerus. Vet. Rec. 90, 577.

Chong, K., et al. (1969). Propagation of axially symmetric waves in hollow elastic circular cylinders subjected to a step function loading. J. Acoust. Soc. Amer. 49, 1, 201-210.

Chou, S. and Greif, R. (1968). Numerical solution of stress waves in layered media. AIAA J. 6, 6, 1067-1073.

Chree, C. (1889). The equations of an isotropic elastic solid in polar and cylindrical coordinates, their solution and application. Trans. Cambridge Phil. Soc. 14, 250.

Clemedson, C. and Jönsson, A. (1961). Transmission and reflection of high explosive shock waves in bone. Acta Physiol. Scand. 51, 47-61.

Cochran, G. (1972). Implantation of strain gages in bone in vivo. J. Biomech. 5, 119-123.

Cochran, G. (1974). A method for direct recording of electromechanical data from skeletal bone in living animals. J. Biomech. 7, 563-565.

Cooper, W. (1970). A communication network approach to sub-millimetric wave techniques in nondestructive testing. Research Techniques in Nondestructive Testing (Ed. by R. Sharpe) Academic Press, N.Y. 315-344.

Crafts, R. (1966). A Textbook of Human Anatomy. Ronald Press Co., N.Y.

Currey, J. (1954). Differences in the tensile strength of bone of different histological types. J. Anat. 93, 87-95.

Currey, J. (1959). Differences in the tensile strength of bone of different histological types. J. Anat. 93, 87.

Currey, J. (1964). Three analogies to explain the mechanical properties of bone. Biorheology 2, 1-10.

Currey, J. (1968). The adaptation of bones to stress. J. Theoret. Biol. 20, 91-106.

Currey, J. (1969a). The mechanical consequences of variation in the mineral content of bone. J. Biomech. 2, 1-11.

Currey, J. (1969b). The relationship between the stiffness and the mineral content of bone. J. Biomech. 2, 477-480.

Currey, J. (1970). The mechanical properties of bone. Clin. Orth. 73, 210-231.

Currey, J. (1975). The effects of stress rate, reconstruction and mineral content in some mechanical properties of bovine bone. J. Biomech. 8, 81-86.

Dalen, N. and Alvestrand, A. (1973). Bone mineral content in chronic renal failure and after renal transplant. Clin. Orth. 1, 6, 338-346.

Dalen, N. and Edsmyr, R. (1974). Bone mineral content of the femoral neck after irradiation. Acta Radiol. 13, 2, 97-101.

Dalen, N. and Feldreich, A. (1974). Osteopenia in alcoholism. Clin. Orth. and Related Res., 201-206.

Dalen, N. and Lamke, B. (1974). Grading of osteoporosis by skeletal roentgenology and bone scanning. Acta Radiol. 15, 177-186.

Dalen, N. and Olsson, K. (1974). Bone mineral content and physical activity. Acta Orth. Scand. 45, 170-174.

Davis, R. (1948). A critical study of the hopkinson pressure bar. Trans. Roy. Phil. Soc. London 240, 375-457.

Dempster, W. and Coleman, R. (1961). Tensile strength of bone along and across the grain. J. Appl. Physiol. 16, 355.

Dempster, W. and Liddicoat, R. (1952). Compact bone as a nonisotropic material. Amer. J. Anat. 91, 331.

Doherty, W., et al (1974). Evaluation of the use of resonant frequencies to characterize physical properties of human long bones. J. Biomech. 7, 559-561.

Doyle, D. (1968). Age related bone changes in women. Progress in Methods of Bone Mineral Measurements. U.S. Dept. of H.E.W., 115-133.

Duthie, R. and Hoaglund, F. (1974). Generalized bone disorders. Principles of Surgery (Ed. by S. Schwartz). McGraw-Hill, N.Y.

Edwards, P and Nilsson, B. (1965). Graphic representation of healing time fractures of the shaft of the tibia. Acta orthop. Scand. 36, 104-111.

Efron, L. and Malvern, L. (1969). Electromagnetic velocity transducer studies of plastic waves in aluminum bars. Exp. Mech., June, 255-262.

Ellis, H. (1958). The speed of healing after fracture of the tibial shaft. J.B.J.S. 40B, 42-46.

Enlow, D. (1966). An evaluation of the use of bone histology in forensic medicine and anthropology. Studies on the Anatomy and Function of Bone and Joints (Ed. by F. Evans), Springer-Verlag, N.Y., 93-112.

Evans, F. (1957). Stress and Strain in Bones. C. C. Thomas, Springfield, Illinois.

Evans, F. (1958). Relations between the microscopic structure and tensile strength of human bone. Acta Anat. 35, 285-301.

Evans, F. (1969). Relation of collagen fiber orientation to some mechanical properties of human cortical bone. J. Biomech. 2, 63-71.

Evans, F. (1973). Mechanical Properties of Bone. C. C. Thomas, Springfield, Illinois.

Evans, F. (1974). Age changes in mechanical properties of human bone. Proc. 11th Ann. Meeting Soc. Engng. Sci., 186-187.

Evans, F. and Bang, S. (1966). Physical and histiological differences between human fibular and femoral compact bone. Studies on the Anatomy and Function of Bone and Joints. (Ed. by F. Evans), Springer-Verlag, N.Y., 142-155.

Evans, F. and Bang, S. (1967). Differences and relationships between the physical properties and the microscopic structure of human femoral, tibial and fibular cortical bone. Amer. J. Anat. 120 1, 79-88.

Evans, F. and Lebow, M. (1951). Regional differences in some of the physical properties of the human femur. J. Appl. Physiol. 3, 563.

Evans, F. and Vincentelli, R. (1969). Relation of collagen fiber orientation to some mechanical properties of human cortical bone. J. Biomech. 2, 63-71.

Evans, F. and Vincentelli, R. (1974). Relations of the compressive properties of human cortical bone to histological structure and calcification. J. Biomech. 7, 1-10.

Fellenbaum, S. and Jonas, S. (1968). Bilateral fractures of the radius and ulna of a dog repaired with Jonas splints. J.A.V.M.A. 152, 4, 365-369.

Fitch, A. (1963). Observation of elastic pulse propagation in axial xymmetric and nonaxially symmetric longitudinal modes of hollow cylinders. J. Acoust. Soc. Amer. 35, 5, 706-708.

Floriani, L, et al. (1967). Mechanical properties of healing bone by the use of ultrasound. Surg. Forum 18, 468-479.

Frankel, V. (1960). The Femoral Neck. Almquist and Wiksell, Uppsala. Diss. Upsala.

Friedenberg, Z. and French, G. (1951). The effects of known compression forces on fracture healing. Surg., Gyn. and Obs. 94, 743-748.

Frost, H. (19). Pyogenic osteomyelitis: the influence of bone remodeling on recurrence. 42-48.

Frost, H. (1963). Bone Remodeling dynamics. C. C. Thomas Co., Springfield, Illinois.

Frost, H. (1964). The Laws of Bone Structure. C. C. Thomas Co., Springfield, Illinois.

Frost. H. (1973). Orthopaedic Biomechanics. C. C. Thomas Co., Springfield, Illinois.

Garner, E. and Blukketter, D. (1975). In vivo determination of macroscopic biological material properties. J. Appl. Mech., Trans. ASME, 350-355.

Gazis, D. (1959). Three dimensional investigation of the propagation of waves in hollow circular cylinders. I. Analytic foundation. J. Acoust. Soc. Amer. 31, 5, 568-572.

Gazis, D. (1959). Three dimensional investigation of waves in hollow circular cylinders. II. Numerical Results. J. Acoust. Soc. Amer. 31, 5, 573-578.

Gjelsvik, A. (1973). Bone remodeling and piezoelectricity I. J. Biomech. 6, 69-77.

Gjelsvik, A. (1973). Bone remodeling and piezoelectricity II. J. Biomech. 6, 187-193.

Glimcher, M. (1974). Studies of the structure, organization and reactivity of bone collagen. Proc. Inter. Symp. on Wound Healing.

Goodier, J., et al. (1959). An experimental surface wave method for recording force-time curves in elastic impacts. J. Appl. Mech., Trans. ASME, 3-7.

Grenoble, D., et al. (1972). The elastic properties of hard tissues and apatites. J. Biomed. Mater. Res. 6, 221-233.

Guyton, A. (1971). Textbook of Medical Physiology. 4th ed. W. B. Saunders Co., Philadelphia.

Habberstad, J. (1971). A two dimensional numerical solution for elastic waves in variously configured rods. J. Appl. Mech., Trans. ASME, 62-70.

Habberstad, J. and Hoge, K. (1971). Effects of a discontinuity in cross section on an elastic pulse. J. Appl. Mech., Trans. ASME, 280-282.

Habbloobl, S. (1972). Strain gage techniques for cadaveric bone. Engng. Med. 1, 2, 36-47.

Handelman, G. and Rubenfeld, L. (1972). Wave propagation in a finite length bar with variable cross section. J. Appl. Mech., Trans. ASME, 278-280.

Hardy, C. and Marcal, P. (1973). Elastic analysis of a skull. J. Appl. Mech., Trans ASME, 1-5.

Hassler, C., et al. (1973a). Effects of quantitative compressive load upon bone healing and quantitative bone blood flow in rabbit calvaria. Proc. 26th ACEMB Conf.

Hassler, C., et al (1973b). An investigation of optimal compressive loading. Proc. ASME Conf. - 1973.

Henneke, E. (1972). Reflection-refraction of a stress wave at a plane boundary between anisotropic media. J. Acoust. Soc. Amer. 51, 1, 210-217.

Henry, A., et al. (1968). Studies on the mechanical properties of healing experimental fractures. Proc. Soc. Med. 61, 902-906.

Herring, G. (1964). Chemistry of the bone matrix. Clin. Orthop. 36, 169-183.

Herring, G. (1968). The chemical structure of tendon, cartilage, dentin and bone matrix. Clin. Orthop. 60, 261-299.

Herrmann, G. and Liebowitz, H. (1972). Mechanics of bone fracture. Fracture: An Advanced Treatise (Ed. by H. Liebowitz), Academic Press, N.Y., 771-840.

Herrmann, G. and Mirsky, I. (1956). Three dimensional and shell theory analysis of axially symmetric motions of cylinders. J. Appl. Mech., 563.568.

Herold, H., et al. (1969). Cartilage extracts in treatment of fractures in rabbits. Acta Orth. Scand. 40, 317-324.

Hert, J., et al. (1965). Comparison of the mechanical properties of both the primary and Haversian bone tissue. Acta Anat. 61, 412-423.

Hicks, J. (1973). The fixation of fractures using plates. Engng. Med. 2, 3, 60-63.

Hirsch, C. and Evans, F. (1965). Studies on some physical properties of infant compact bone. Acta Orthop. Scand. 35, 300.

Hoaglund, F. and States, J. (1967). Factors influencing the rate of healing in tibial shaft fractures. Surg., Gyn. and Obs. 124, 1, 71-76.

Hoffman, R., et al. (1968). Computed shock response of porous aluminum. J. Appl. Phy. 39, 10, 4555-4562.

Hohn, R. (1973). Plate fixation of comminuted femoral shaft fractures in the dog. J.A.V.M.A. 162, 8, 646-647.

Horn, C. and Robinson, D. (1965). Assessment of fracture healing by ultrasound. J. Coll. Radiol. Aust. 9, 165.

Hornby, I. and Noltingk, B. (1973). The application of the vibrating wire principle for the measurement of strain in concrete. Proc. 1973 SESA Meeting, 1-11.

Hsu, F. (1968). The influence of mechanical loads on the form of a growing elastic body. J. Biomech. 1, 303-311.

Jankovich, J. (1972). The effects of mechanical vibration on bone development in the rat. J. Biomech. 5, 241-250.

Jendrucko, R., et al. (1974). Matrix deformation and stress induced pressure development in bone cells. Proc. 11th. Ann. Meeting Soc. Engng. Sci., 192-193.

Jones, J. (1961). Rayleigh waves in a porous elastic saturated solid. J. Acoust. Soc. Amer. 33, 7, 959-962.

Jones, J. (1969). Pulse propagation in a poroelastic solid. J. Appl. Mech., Trans. ASME, 878-880.

Jurist, J. (1970a). In vivo determination of the elastic response of bone. I. Method of ulnar resonant frequency determination. Phy. Med. Biol. 15, 3, 417-426.

Jurist, J. (1970b). In vivo determination of the elastic response of bone. II. Ulnar resonant frequency in osteoporotic, diabetic and normal subjects. Phy. Med. Biol. 15, 3, 427-434.

Jurist, J. (1971). Correspondence, Phy. Med. Biol. 16, 1, 149-150.

Jurist, J. (1972). Correspondence, Phy. Med. Biol. 17, 290-291.

Jurist, J. and Kianian, K. (1973). Three models of the vibrating ulna. J. Biomech. 6, 331-342.

Justus, R. and Luft, J. (1970). A mechanochemical hypothesis for bone remodeling induced by mechanical stress. Calc. Tiss. Res. 5 222-235.

Katz, J. (1971). Hard tissue as a composite material I. Bounds on the elastic behavior. J. Biomech. 4, 455-473.

Katz, J., et al. (1974). Torsional and biaxial viscoelastic response in cortical bone. Proc. 11th. Ann. Meeting Soc. Engng. Sci., 188-189.

Katz, J. and Ukraincik, K. (1971). On the anisotropic elastic properties of hydroxyapatite. J. Biomech. 4, 221-227.

Kazarian, L. and von Gierke, H. (19). The effects of hypogravic and hypodynamic environments on the skeletal system and acceleration tolerance. 475-499.

Keane, B., Spiegler, G. and Davis, R. (1959). Quantitative evaluation of bone mineral by a radiographic method. Brit. J. Radiol. 32, 162-167.

Kennedy, L. and Jones, O. (1969). Longitudinal wave propagation in a circularly bar loaded suddenly by a radially distributed end stress. J. Appl. Mech., Trans. ASME, 470-478.

Kenner, V. and Goldsmith, W. (1968). One dimensional wave propagation through a short discontinuity. J. Acoust. Soc. Amer. 45, 1, 115-118.

Kenner, V. et al. (1975). Dynamic measurements of elastic properties for compact bone. Proc. 1975 Appl. Mech. Conf., 129-131.

King, T. (1957). Compression of the bone ends as an aid to union in fractures. J.B.J.S. 39-A, 1238-1248.

Klima, S., et al. (1965). Applications of ultrasonics to detection of fatigue cracks. Proc. 2nd. SESA Inter. Cong. Exp. Mech. (Ed. by B. Rossi) Pergamon Press. N.Y., 320-327.

Knese, K. (1958). Knockenstruksur als verbundbau Theime, Stutgart.

Ko, R. (1953). J. Kyoto Pref. Med. Univ. 53, 503-525.

Kolsky, H. (1963). Stress Waves in Solids. Dover Publ, Inc., N.Y.

Kolsky, H. (19). The detection and measurement of stress waves. Exp. Tech. Shock Vib. 11-24.

Kolsky, H. (1974). Some recent experimental investigations in stress wave propagation and fracture. Dynamic response of structures. (Ed. by G. Herrmann and N. Perrone). Pergamon Press, Inc., 327-343.

Kranendonk, D., et al. (1972). Femoral trabecular patterns and bone mineral content. J. Bone Joint Surg. 54-A, 7, 1472-1478.

Lachmann, E. (1955). Osteoporosis: the potentialities and limitations of its roentgenologic diagnosis. Amer. J. Roentgenology 74, 712-715.

Lachmann, E. and Whelan, M. (1936). The roentgen diagnosis of osteoporosis and its limitations. Radiology 26, 165-177.

Laird, G. and Kingsbury, H. (1973). Complex viscoelastic moduli of bovine bone. J. Biomech. 6, 59-67.

Lang, S. (1969). Science 165, 287-288.

Lang, S. (1970). Ultrasonic method for measuring elastic coefficients of bone and results on fresh and dried bovine bones. IEEE Trans. Biomed. Engng. 17, 2, 101-105.

Lanyon, L. (1971). Strain in sheep lumbar vertebrae recorded during life. Acta Orth. Scand. 42, 102-112.

Lanyon, L. (1973). Analysis of surface bone strain in the calcaneus of sheep during normal locomotion. J. Biomech. 6, 41-49.

Lee, T. and Sechler, E. (1975). Longitudinal waves in wedges. Exp. Mech., 41-48.

Leedale, A. and Quigley, P. (1972). Open reduction repair of fractures of the distal shaft of the humerus in the dog: a report of 13 cases. Vet. Rec. 90, 419-424.

Lewis, J. and Goldsmith, W. (1975). The dynamic fracture and prefracture response of compact bone by split Hopkinson bar methods. J. Biomech. 8, 27-40.

Lightowler, C. and Swanson, S. (1972). Recovery of strength in healing experimental fractures. Proc. Roy. Soc. Med. 65, 738-739.

Lindsay, M. and Howes, E. (1931). The breaking strength of healing fractures. J.B.J.S. 13A, 491-501.

Lissner, H. and Roberts, V. (1966). Evaluation of skeletal impacts of human cadavers. Studies Anat. Func. 113-120.

Ljunggren, G. (1971). Fractures in the dog. Clin. Orth. Related Res. 81, 158-164.

Lubinski, A. (1955). The theory of elasticity for porous bodies displaying a strong pore structure. Proc. 2nd. U.S. Nat. Cong. Appl. Mech., 247-256.

Lugassy, A. and Korostoff, E. (1969). Viscoelastic behavior of bovine femoral cortical bone and sperm whale dentin. Res. Dent. Med. Mater. Plenum Press, 1-17.

Mack, R. (1964). Bone - a natural two phase material. Tech. Mem., Biomech. Lab. U.C.S.F., Berkeley.

Maj, G. (1938). Osservazioni sulle differeze kopographiche della resistenza meccanica del tessuto osseo di uno stesso segmento scheletrico. Monitore Zool. Ital., 49, 139-149.

Mallik, A. and Ghosh, A. (1974). Damping characteristics of composite and porous materials. J. Composite Mater. 8, 207-211.

Martin, R. and Advani, S. (1974). Constitutive expressions for bone and their relation to pathophysiology. Proc. 11th. Ann. Meeting Soc. Engng. Sci., 180-181.

Mather, B. (1967). The symmetry of the mechanical properties of the human femur. J. Surg. Res. 7, 222.

Mather, B. (1968). Observations on the effects of static and impact loading on the human femur. J. Biomech. 1, 331-335.

McElhaney, J. (1966). Dynamic response of bone and muscle tissue. J. Appl. Physiol. 21, 1231.

McElhaney, J. and Byars, E. (1965). Dynamic response of biological materials. ASME paper No. 65-WA/HUF-9.

McElhaney, J. and Byars, E. (1965). Effect of embalming on the mechanical properties of beef bone. J. Appl. Physiol. 19, 1234.

McNiven, H. and Mingi, Y. (1972). Transiet response in a rod in terms of power series expansion. J. Sound Vib. 21, 1, 11-18.

Meema, H., Harris, C. and Porrett, B. (1964). A method for determination of bone salt content of cortical bone. Radiology 82, 986-997.

Melnick, R. and Miller, D. (1966). Variations of tensile strength of human cortical bone with age. Clin. Sci. 30, 243.

Miklowitz, J. (1957). The propa-ation of compressional waves in a dis-perssive elastic rod. Pt. I. - Results from the theory. J. Appl. Mech., 231-239.

Miklowitz, J. and Nisewanger, C. (1957). The propagation of compressional waves in a disperssive elastic rod. Pt. II - Exp. results and comparison with theory. J. Appl. Mech., 240-244.

Mindlin, R. and Herrman, G. (1951). A one dimensional theory of compressional waves in an elastic rod. Proc. 1st. U.S. Nat. Cong. Appl. Mech., 187-191.

Moldawer, M. (1963). Osteoporosis in restorative medicine in geriatrics. (Ed. by M. Dacso) C. C. Thomas, Springfield, Illinois, 170.

Niemeyer, K. and Hoeffer, R. (1971). Rush pin repair of distal fractures of long bones in the dog. J.A.V.M.A., 159, 11, 1433-1434.

Nilsson, B. and Edwards, P. (1969). Age and fracture healing. Geriatrics 24, 112-117.

Nowinski, J. (1970). Cylindrical bones as anisotropic poroelastic members subjected to hydrostatic pressure. Proc. 5th. S.E. Conf. Theoret. Appl. Mech.

Nowinski, J. (1971). Bone articulations as systems of poroelastic bodies in contact. AIAA J. 9, 62-67.

Nowinski, J. (1972). Stress concentration around a cylindrical cavity in a bone treated as a poroelastic body. Acta Mech. 13, 281-292.

Nowinski, J. (1973). Bielayev's point in poroelastic bodies in contact. Inter. J. Mech. Sci. 15, 145-155.

Nowinski, J. and Davis, C. (1971). Propagation of longitudinal waves in circularly cylindrical bone elements. J. Appl. Mech., 578-584.

Nowinski, J. and Davis, C. (1972). The flexure and torsion of bones viewed as anisotropic poroelastic bodies. Inter. J. Engng. Sci. 10, 1063-1079.

Patten, B. (1968). Human Embryology. 3rd. ed., Mcgraw-Hill, N.Y.

Pearson, C. (1959). Theoretical Elasticity. Harvard Univ. Press. Cambridge, Massachusetts.

Pelker, R. and Saha, S. (1975). A theoretical investigation of wave propagation in long bones. 1975 Advances in Bioengineering (Ed. by A. Bell and R. Nerem). ASME, N.Y., 98-100.

Pernica, G. and McNiven, H. (1973). Comparison of experimental and theoretical responses in hollow rods to a transient input. J. Acoust. Soc. Amer. 53, 5, 1365-1376.

Piekarski, K. (1970). Fracture of bone. J. Appl. Phy. 41, 1, 215-223.

Piekarski, K. (1973). Analysis of bone as a composite material. Inter. J. Engng. Sci. 11, 557-565.

Piekarski, K., et al. (1969). The effect of delayed internal fixation on fracture healing. Acta Orth. Scand. 40, 543-551.

Pochhammer, L. (1876). Uber Fortpflanzungzungsgesch-windigkeiten kleiner Schwingungen in einem unbegrenzten isotropen Kreiszylinder. J. f. reine u. angew. Math. 81, 324.

Pope, M. and Outwater, J. (1974). Mechanical properties of bone as a function of position and orientation. J. Biomech. 7, 61-66.

Posner, A., et al. (1963). Arch. Oral Biol. 8, 549.

Powell, T. and Valentinuzzi, M. (1974). Calcium homeostasis: responses of a possible mathematical model. Med. Biol. Engng., May, 287-294.

Pugh, J., et al. (1973). Mechanical resonance spectra in human cancellous bone. Science 181, 271-272.

Pukl, J., et al. (1972). Biomechanical properties of paired canine fibulas. J. Biomech. 5, 391-397.

Reuter, R. (1968). Dispersion of flexural waves in circular biomaterial cylinders-theoretical treatment. J. Acoust. Soc. Amer. 46, 3, 643-648.

Rich, C., et al. (1966). Measurement of bone mass from ultrasonic transmission time. Proc. Soc. Exp. Bio. Med. 123, 282-285.

Rickards, D., et al. (1972). Orthopedic procedures for laboratory animals and exotic pets. J.A.V.M.A. 161, 728-732.

Ripperger, E. and Yeakley, L. (1963). Measurement of particle velocities associated with waves propagating in bars. Exp. Mech., Feb. 47-56.

Roberts, V. (1965). Strain gage techniques in biomechanics. Proc. 2nd. SESA Inter. Conf. Exp. Mech., 339-342.

Robinson, R. (1960). Crystal-collagen-water relationships in bone matrix. Clin. Orth. 17, 69.

Rothman, R. (1967). Electrical and mechanical principles in bone biodynamics. Engng. in the Practice of Medicine. (Ed. by B. Segal). Williams and Wilkins Co., Baltimore, 142-147.

Rybicki, E., et al. (1972). On the mathematical analysis of stress in the human femur. J. Biomech. 5, 203-215.

Rybicki, E., et al. (1974). Mathematical and experimental studies on the mechanisms of plated transverse fractures. J. Biomech. 7, 377-384.

Rybicki, E., et al. (19). Use of computer generated movies for studying the mechanics of bone plate fixation.

Saha, S. (1973). Anisotropic analysis of bone - some two dimensional problems. J. Biomech. 6, 641.

Saha, S. (1974). Dynamic strength of human compact bone as a function of its microstructure. Proc. 27th ACEMB 290.

Saha. S. and Hayes, W. (1974). Instrumented tensile impact tests of bone. Exp. Mech. 14, 12 473-478.

Saha, S. and Hayes, W. (1976). Tensile impact properties of human compact bone. J. Biomech. 9, 243-251.

Saha, S. and Pelker, R. (1975). Stress wave propagation in bone. Proc. 28th ACEMB, 172.

Saha, S. and Pelker, R. (1976). Measurement of fracture healing by the use of stress waves. Proc. 1976 O.R.S.

Salmons, S. (1975). In vivo tenson tension and bone strain measurement and correlation. J. Biomech. 8, 87.

Schenck, T. and Somerset, J. (1969). Stresses in orthopedic walking casts. J. Biomech. 2, 227-239.

Schwartz, S. (1974). Principles of Surgery. 2nd ed. McGraw-Hill, N.Y.

Sedlin, E. (1965). A rheological model for cortical bone. Acta Orth. Scand. 36, Suppl. 83.

Sedlin, E. and Hirsch, C. (1966). Factors affecting the determination of the physical properties of femoral cortical bone. Acta Orthop. Scand. 37, 29.

Selle, W. and Jurist, J. (1966). Acoustical detection of senile osteoporosis. Proc. Soc. Exp. Biol. Med. 121, 150-152.

Smith, J. and Walmsley, R. (1959). Factors affecting the elasticity of bone. J. Anat. 93, 503.

Solomon, F. and Hassan, S. (1964). Serum calcium and phosphorus in rabbits during fracture healing, with reference to parathyroid activity. Nature, 204, 693-694.

Stech, E. (1967). A descriptive model of lamellar bone anisotropy. Amer. Soc. Mech. Engng. Monograph, paper No. 66-HUF-3, 236-245.

Sve, C. (1973). Elastic wave propagation in a porous laminated composite. Inter. J. Solids Structure 9, 937-950.

Swanson, S. (1971). Biomechanical characteristics of bone. Advances in Biomedical Engineering. Academic Press, N.Y., 137-187.

Tanaka, K. and Kurokawa, T. (1973). Stress wave propagation in a bar of variable cross section. Bull. J.S.M.E. 16, 93, 485-491.

Tennyson, R., et al. (1972). Dynamic viscoelastic response of bone. Exp. Mech., 502-507.

Thompson, G., et al. (19). Determination of mechanical properties of excised dog radius from lateral vibration experiments.

Thompson, G. (1973). In vivo determination of bone properties from mechanical impedance measurements. Aerospace Med. Assoc. Ann. Sci. Meeting Abstracts.

Timoshenko, S. and Goodier, J. (1970). Theory of Elasticity. 3rd. ed. McGraw-Hill, N.Y.

Toajari, E. (1938). Resistenza meccanica ed elastica del tessuto osseo studiata in rapporto alla meniche structtura. Monit. Zool. Ital. 48.

Toridis, T. (1969). Stress Analysis of the Femur. J. Biomech. 2, 163-174.

Trofimov, V. (1968). Anomalous shock compressibility of porous materials. Fizika Gorenija i Vzrva 4, 2, 244-253.

Uhthoff, H. and Dubuc, F. (1971). Bone structure changes in the dog under rigid internal fixation. Clin. Orth. Rel. Res., 165-170.

Vayo, H. W. and Ghista, D. N. (1971). Wave propagation in bone media. Bull. Math. Biophysics 33, 463-479.

Vincentelli, R. and Evans, F. (1971). Relations among mechanical properties, collagen fibers and calcification in adult human cortical bone. J. Biomech. 4, 193-201.

Vose, C. (1962). The relationship of microscopic mineralization to intrinsic bone strength. Anat. Rec. 144, 1, 31-36.

Vose, G. (1974). Review of roentgenographic bone demineralization studies of the Gemini space flights. Amer. J. Roentgenology, Rad. Therapy, and Nuc. Med. 121, 1, 1-4.

Vose, G. and Kubula, A. (1959). Bone strength - its relationship to x-ray determined ash content. Human Biol. 31, 262-270.

Vose, G. and Mack, P. (1963). Roentgenologic assessment of femoral neck density as related to fracturing. Amer. J. Roent., Rad. Nuc. Med. 89, 6, 1296-1301.

Walnut, T. (1967). A mathematical analysis of the changes in the size and shape of bones during growth, 31, 217-230.

Wertheim, M. (1847). Memoire sur l'elasticite et la cohesion des principaux tissues du corps humain. Ann. Chem. Phy., Paris, 21, 385-414.

White, A., et al. (1974). Analysis of mechanical symmetry in rabbit long bones. Acta Orth. Scand. 45, 328-336.

Whittier, J. and Jones, J. (1967). Axially symmetric wave propagation in a two layered cylinder. Inter. J. Solids Structures 3, 657-675.

Wong, P., et al. (1966). Propagation of harmonic waves in an infinite elastic rod of elliptical cross section. J. Acoust. Soc. Amer. 40, 2, 393-398.

Wood, J. (1971). Dynamic response of human cranial bone. J. Biomech. 4, 1-12.

Wu, C. and Sackman, J. (1974). One dimensional wave propagation in semi linear viscoelastic media. Inter. J. Non-Linear Mech. 9, 521-528.

Yamada, H. (1970). The Strength of Biological Materials. (Ed. by F. Evans.) Williams and Wilkins, Baltimore.

Yamagishi, M., et al. (1955). The biomechanics of fracture healing. J. Bone Joint Struct. 37-A, 5, 1035-1068.

Yohoo, S. (1952). J. Kyoto Pref. Med. Univ. 51, 291-313.

Yuan, H. and Lianis, G. (1974). Experimental investigation of wave propagation in nonlinear viscoelastic materials. Rheol. Acta 13, 40-48.